T.R.
GEBZE TECHNICAL UNIVERSITY
GRADUATE SCHOOL

EFFECT OF PYK GENE DELETIONS ON SHIKIMIC ACID PATHWAY IN PSEUDOMONAS PUTIDA

HATİCE ARSLAN

A THESIS OF MASTER OF SCIENCE
DEPARTMENT OF MOLECULAR BIOLOGY AND GENETICS

ADVISOR: ASSOC. PROF. ÖZLEM AKKAYA

NOVEMBER 2024

T.R.
GEBZE TECHNICAL UNIVERSITY
GRADUATE SCHOOL

EFFECT OF PYK GENE DELETIONS ON SHIKIMIC ACID PATHWAY IN PSEUDOMONAS PUTIDA

HATİCE ARSLAN

A THESIS OF MASTER OF SCIENCE
DEPARTMENT OF MOLECULAR BIOLOGY AND GENETICS

ADVISOR: ASSOC. PROF. ÖZLEM AKKAYA

NOVEMBER 2024

T.C.
GEBZE TEKNİK ÜNİVERSİTESİ
LİSANSÜSTÜ EĞİTİM ENSTİTÜSÜ

PSEUDOMONAS PUTİDA'DA PYK GENLERİNİN SİLİNMESİNİN ŞİKİMİK ASİT YOLAĞI ÜZERİNDEKİ ETKİSİ

HATİCE ARSLAN

YÜKSEK LİSANS TEZİ
MOLEKÜLER BİYOLOJİ VE GENETİK ANABİLİM DALI

DANIŞMAN: DOÇ. DR. ÖZLEM AKKAYA

KASIM 2024

MASTER of SCIENCE JURY APPROVAL FORM

A thesis submitted by Hatice ARSLAN defended on 01/11/2024 before the jury formed with the 29/07/2024 date and 2024/42 numbered decision of the GTU Graduate Administration Board, has been accepted as a MASTER of SCIENCE thesis in the Department of Molecular Biology and Genetics.

JURY

MEMBER
(THESIS ADVISOR) : Assoc. Prof. Özlem AKKAYA

MEMBER : Assoc. Prof. Fatma İnci ÖZDEMİR

MEMBER : Prof. Dr. Mehmet ÖZTÜRK

APPROVAL

Gebze Technical University Graduate Administration Board

…..…/…..…/..…… date and ……/…….. numbered decision.

SIGNATURE/SEAL

ABSTRACT

Shikimic acid (SA) serves as a key intermediate in the shikimate pathway, which is found in both bacteria and plants. The shikimic acid pathway synthesizes essential vitamins and aromatic amino acids (AAA) like phenylalanine, tyrosine, and tryptophan. SA acts as an intermediate compound in the biosynthesis of AAA and serves as a precursor for the chemical synthesis of oseltamivir phosphate (Tamiflu), a drug used to treat influenza. Furthermore, many secondary metabolites such as gallic acid, muconic acid, salicylic acid, and anthranilic acid are produced through the SA pathway. Since these metabolites are widely utilized in the pharmaceutical, cosmetic, and food industries, various organisms are used in these sectors to reduce costs and achieve eco-friendly manufacturing.

Pseudomonas putida (*P. putida*) is preferred as a chassis in synthetic biology and metabolic engineering research due to its capacity to harbor pathways designed to produce valuable chemicals or degrade/valorize environmental pollutants. In this study, we investigated the effect of pyruvate kinase (*pyk*) genes on metabolic flux to the AAA pathway. For this purpose, the *P. putida* genome was edited, and *pyk* genes were deleted using the I-*Sce*I method. The effect of *pyk* gene deletions on bacterial growth, glucose consumption, and metabolic flux towards the SA pathway was investigated in a *P. putida* EM42 strain with a *hexR*-deleted gene. The results demonstrated that introducing *pykA* deletion into the *hexR* gene knockout strain led to a decrease in both growth rate and glucose consumption. Moreover, metabolite analysis results indicate that the deletion of *pykA* plays a more dominant role compared to *pykF* in increasing the flux towards the shikimate pathway. Due to the lack of detailed research on comparing *pyk*s in *P. putida*, this research will contribute to the literature by elucidating the role of *pyk* genes in the metabolic flux towards the phosphoenolpyruvate (PEP).

Keywords: *Pseudomonas putida*, Pyruvate Kinase, Shikimic Acid Pathway, Metabolic Engineering, Synthetic Biology

ÖZET

Şikimik asit (SA), hem bakterilerde hem de bitkilerde bulunan şikimat yolağında yer alan önemli bir ara metabolittir. Şikimik asit yolağı temel vitaminler, fenilalanin, tirozin ve triptofan gibi aromatik amino asitleri sentezler. SA, aromatik amino asitlerin (AAA) biyosentezinde bir ara bileşik olarak işlev görür ve influenza tedavisinde kullanılan bir ilaç olan oseltamivir fosfatın (Tamiflu) kimyasal sentezinin öncül maddesi olarak hizmet eder. Ayrıca, gallik asit, mukonik asit, salisilik asit ve antranilik asit gibi birçok ikincil metabolit SA yolağından üretilmektedir. Bu metabolitlerden ilaç, kozmetik ve gıda endüstrilerinde yaygın olarak yararlanıldığından, çeşitli organizmalar söz konusu sektörlerde maliyeti düşürmek ve çevre dostu üretim elde etmek için kullanılmaktadır.

P. putida (*Pseudomonas putida*), değerli kimyasalların üretiminde veya çevresel kirleticilerin degradasyonunda rol oynayan yolakları barındırma kapasitesinden dolayı sentetik biyoloji ve metabolizma mühendisliği araştırmalarında sıklıkla tercih edilen konakçı bir organizmadır. Bu çalışmada, piruvat kinaz (*pyk*) genlerinin şikimik asit yolağına olan metabolik akış üzerine etkisi incelenmiştir. Bu amaçla, *P. putida* genomu düzenlenmiş ve *pyk* genleri I-*Sce*I yöntemi kullanılarak silinmiştir. İlgili delesyonların bakterinin büyümesine, glikoz tüketimine ve SA yolağına doğru olan metabolik akışa etkileri *hexR* geni delesyona uğratılmış *P. putida* EM42 soyunda araştırılmıştır. Sonuçlar, *pykA* delesyonunun bakterinin hem büyüme oranında hem de glikoz tüketiminde yavaşlamaya yol açtığını göstermiştir. Ayrıca, metabolit analiz sonuçları, *pykA* delesyonunun SA yolağına doğru akışın artırılmasında *pykF*'e görece daha baskın rol oynayabileceğine işaret etmiştir. Bu tez çalışması *P. putida*'da *pyk* genlerinin metabolik akışın fosfoenolpiruvat (PEP)'a doğru yönlendirilmesindeki rollerinin açığa kavuşturulması adına literatüre katkı sağlayacaktır.

Anahtar kelimeler: *Pseudomonas putida*, Piruvat Kinaz, Şikimik Asit Yolağı, Metabolizma Mühendisliği, Sentetik Biyoloji

ACKNOWLEDGEMENTS

I would like to thank Associate Professor Özlem AKKAYA, my advisor, for her academic improvement and contributions to me and for sharing her experiences with me.
I would like to express my gratitude to Prof. Dr. Devrim ATİLLA and Assoc. Prof. Dr. Emrah NIKEREL for kindly providing me access to their laboratories to conduct my experiments.
I would like to extend my sincere thanks to my friend Osman Sait AKBAŞ, with whom I conducted many of the experiments tirelessly, day and night; to PhD student Ahmet KALAYCI for sharing his expertise with me; and to my valued lab colleagues: Ömer ASLANTAŞ, Mustafa Eren YILDIZ, Efe AKSOY, Mehmet AKYILDIZ, Melike KARAMAN, Reyhan AYDIN, and Mustafa Batın TEKCAN.
Additionally, I am deeply grateful to my dear friends Hilal KANDEMIR, Meryem ÇETKIN, and Iremnur BAYRAM for their unwavering friendship and continuous support.
I would like to express my deepest appreciation to my beloved mother, Meryem ARSLAN, and father, Ahmet ARSLAN, as well as to my siblings Merve BAKIR, İrfan BAKIR, Mahmut ARSLAN, Canan ARSLAN, Selahattin Miraç ARSLAN, and Muhammed Sıddık ARSLAN, for their unwavering support, both financially and emotionally.
Lastly, the greatest thanks go to my one and only sources of motivation, my dear nephews Akif Emre BAKIR and Ahsen Ela ARSLAN.
This study was supported by Scientific and Technological Research Council of Turkey (TUBITAK) under the Grant Number 120Z407. The authors thank to TUBITAK for their supports.

TABLE OF CONTENTS

LIST of SYMBOLS and ABBREVIATIONS

%	: Percentage
µ	: Growth Rate
µF	: Microfarad
µL	: Microliter
µm	: Micrometer
°C	: Degree Celsius
3D	: Three Dimensional
3MB	: 3-methylbenzoate
ADP	: Adenosine Diphosphate
Amp^R	: Ampicillin Resistance
ATP	: Adenosine Triphosphate
B. subtilis	: *Bacillus subtilis*
bp	: Base Pairs
C	: Carbon
Cm^R	: Chloramphenicole Resistance
dH2O	: Deionized Water
DMSO	: Dimethyl Sulfoxide
DSB	: Double-Strand Break
E4P	: Erythrose 4-Phosphate
E. coli	: *Escherichia coli*
e.g.	: *example gratia*
ED	: Entner-Doudoroff
EDEMP	: Entner-Doudoroff-Embden-Meyerhof-Parnas
EDTA	: Ethylenediaminetetraacetic acid
EMP	: Embden-Meyerhof-Parnas
et al.	: et alii, and others
ETOH	: Ethanol
g	: Gram
h	: Hour
H_2O	: Water
HCl	: Hydrogen Chloride
HPLC	: High Performance/Pressure Liquid Chromatography
I-SceI	: *Saccharomyces cerevisiae* Endonuclease
K_2HPO_4	: Dipotassium Hydrogen Phosphate
kb	: Kilobase Pairs
Km^R	: Kanamycin Resistance
L	: Liter

LB	: Lysogeny Broth
log	: Logarithm
M	: Molar
mg	: Milligram
$MgCl_2$	: Magnesium Chloride
$MgSO_4$	: Magnesium Sulfate
min	: Minutes
mL	: Milliliter
M. tuberculosis	: *Mycobacterium tuberculosis*
mM	: Millimolar
NADPH	: Nicotinamide Adenine Dinucleotide Phosphate
Na_2HPO_4	: Disodium Hydrogen Phosphate
NaCl	: Sodium Chloride
NaOH	: Sodium Hydroxide
ng	: Nanogram
NH_4Cl	: Ammonium Chloride
nm	: Nanometer
OD_{600}	: Optical Density at 600 nm
P. aeruginosa	: *Pseudomonas aeruginosa*
P. putida	: *Pseudomonas putida*
P. taiwanensis	: *Pseudomonas taiwanensis*
PCA	: Protocatechuic Acid
PCR	: Polymerase Chain Reaction
PEP	: Phosphoenolpyruvate
pH	: Potential of Hydrogen
Pyk	: Pyruvate Kinase
pLDDT	: Predicted Local Distance Difference Test
ppm	: Parts Per Million
PPP	: Pentos Phosphate Pathway
PykA	: Pyruvate Kinase A
PykF	: Pyruvate Kinase F
rpm	: Rounds Per Minute
s	: Second
SA	: Shikimic Acid
SOE	: Splicing by Overlap Extension
S. typhimurium	: *Salmonella enterica* Serovar Typhimurium
TAE	: Tris-Acetate-EDTA
TCA	: Tricarboxylic Acid
Tn7	: Transposon
TS1	: Target Sequence 1
TS2	: Target Sequence 2

TSS	: Transformation and Storage Solution
UV	: Ultraviolet
V	: Volt
WT	: Wildtype
xylS	: Transcriptional Regulator XylS of *XylS/Pm* Regulator/Promoter System
Y. pestis	: *Yersinia pestis*

LIST OF FIGURES

LIST OF TABLES

1. INTRODUCTION

To enhance economic, social, and environmental sustainability, it is essential to support the development of bio-based products to reduce dependence on fossil fuels. Many chemicals currently in use are derived from petroleum, natural gas, or coal, and the production processes for these chemicals are often characterized by high inefficiencies and significant environmental impacts. Addressing these challenges requires innovative approaches, and microorganisms with well-characterized metabolism and cellular structures have emerged as viable cellular factories for the production of valuable chemicals [Yu, 2017].

Aromatic compounds and their derived chemicals are important in various industrial applications, including the production of polymers, food additives, pharmaceuticals, aromatic flavorings, and biofuels. Considering the unsustainability of fossil resources, the environmental challenges they present, as well as the growing demand for valuable aromatics and chemical compounds sourced from renewable carbohydrate substrates, microbial production has become an increasingly attractive alternative [Li et al., 2020].

In recent years, the utilization of microorganisms as cellular factories for the production of essential metabolites has received significant interest in sustainable production. These microorganisms primarily generate aromatic compounds through the shikimic acid (SA) pathway and aromatic amino acid (AAA) pathways. The SA pathway is characterized by a series of seven biochemical reactions, which initiate with the condensation of phosphoenolpyruvate (PEP) and erythrose 4-phosphate (E4P). The name of the SA pathway derives from shikimic acid, which is the key metabolite produced by this pathway [Li et al., 2020].

SA acts as a pharmaceutical precursor for anti-viral and anti-cancer drugs such as the neuraminidase inhibitor oseltamivir phosphate (Tamiflu®) [Rawat et al., 2013]. Furthermore, the final product of the SA pathway, chorismate, serves as a precursor for the synthesis of aromatic acids and value-added chemicals including cinnamic acid, salicylic acid, folic acid, p-coumaric acid, etc. These compounds have extensive

applications in industries ranging from pharmaceuticals to agriculture and food production [Yu, 2017].

Improved microbial production can be achieved by employing multiple disciplines such as synthetic biology, metabolic engineering, molecular biology, and advanced biotechnology. Through the principles of synthetic biology, microorganisms can be engineered at the genetic level to optimize the biosynthesis of target compounds thereby increasing production rates and efficiency. Metabolic engineering allows for the modification of metabolic pathways to enhance precursor availability and improve the overall yield of desired products.

By leveraging these advanced methodologies and the inherent capabilities of microorganisms, it is possible to establish more sustainable production systems that not only meet the increasing demand for aromatic compounds but also contribute to a more environmentally friendly and economically viable future.

1.1. Aim, Content, and Contribution of Thesis

Pyruvate kinases (Pyks) catalyze the last stage of glycolysis, converting PEP into pyruvate while generating ATP. Pyruvate, the end product of this reaction, serves as a key metabolic intermediate, feeding into multiple pathways, including the citric acid cycle for energy production, fermentation processes under anaerobic conditions, and biosynthetic routes for amino acids and fatty acids. Therefore, Pyk enzymes are essential to modulate broader metabolic networks. In addition, PEP from the Embden-Meyerhof Parnas Pathway (EMPP) and E4P from the Pentose Phosphate Pathway (PPP) were condensed to initiate the SA pathway.

The SA pathway is a vital metabolic route that produces chorismate, a precursor for the AAA: phenylalanine, tyrosine, and tryptophan. The metabolites involved in this pathway possess considerable commercial importance across multiple industrial sectors.

Previous studies have elucidated the impact of *pyk* deletions on the SA pathway in various organisms, such as *Escherichia coli* [Siddiquee et al., 2004], *Pseudomonas aeruginosa* [Abdelhamid, 2019], *Bacillus subtilis* [Fry et al., 2000]. This study will contribute to the

elucidation of the importance of two different *pyk* genes, *pykA* and *pykF*, in *P. putida* EM42Δ*hexR* and the impact of both gene deletions on the metabolic flux towards the shikimate pathway through SA production. The characteristics of these strains were determined under sterile culture conditions. The effects of the deletions on growth rate were examined by monitoring the OD_{600} of these strains over a 72-hour period. A comparison of glucose consumption and pH changes were examined between *P. putida* EM42Δ*hexR,* and *pyk*-deleted *P. putida* EM42Δ*hexR* strains. The effects of deletions on the metabolic flux towards the SA pathway were evaluated by HPLC analysis of SA and DHS production in samples taken at different times of bacterial cultures.

2. LITERATURE SUMMARY

2.1. Metabolic Engineering and Synthetic Biology

While synthetic biology offers the tools and insights into various biological processes, metabolic engineering utilizes this knowledge to enhance the biosynthetic pathway for producing a target compound. These two fields essentially aim to modify DNA by utilizing existing methods, tools, and emerging techniques [García-Granados et al., 2019]. Moreover, synthetic biology focuses on creating novel biological components and enhances the efficiency and functionality of biological systems by designing and optimizing them [Chen et al., 2012]. Metabolic engineering has become a key approach for optimizing industrial fermentation processes by applying recombinant DNA technology to introduce targeted genetic modifications. The process begins with a detailed analysis of cellular functions, followed by the design and construction of an improved strain through genetic engineering. Recent advancements have provided powerful tools for both cellular function analysis and precise genetic modifications. Advances in genomics and bioinformatics have significantly contributed to the field's growth by facilitating genetic engineering and speeding up gene cloning and transformation [Nielsen, 2001].

Moreover, to achieve a cell factory capable of producing cost-effective molecules, a host organism with genetic and physiological advantages should be selected [Zhu et al., 2015]. Additionally, the chassis should be genetically manipulable, safe to culture, and cost-effective to allow for the heterologous expression of genes related to the desired compound synthesis.

In the literature, various organisms are used as a chassis for the production of SA. Metabolic engineering of *Corynebacterium glutamicum* was described to increase the production of SA from glucose. 13.8 g/L was reached as the final titer of SA production [Sato et al., 2020]. In addition, genetic manipulations were constructed to obtain the SA-producing *B. subtilis* strain. Metabolite flux analysis concluded that *B. subtilis* produced 3.46 g/L of SA during batch cultivation of flasks [Liu et al., 2014]. System engineering of

E. coli SA09 was described to achieve the highest titer of shikimate from glucose. The shikimate titer was increased to 126.4 g/L using a bioreactor [Li et al., 2023]. Metabolic engineering of *P. putida* is highly utilized to produce various compounds derived from the SA pathway. In this study, a variant of *P. putida* KT2440 was selected as the chassis.

2.2. *Pseudomonas putida* KT2440

P. putida is a non-pathogenic, rod-shaped, aerobic, gram-negative soil bacterium that is used as a model environmental organism. *P. putida* KT2440 is particularly favored in biotechnology for its capability to produce essential intermediates through metabolic pathways and degrade pollutants [Martins Dos Santos et al., 2004]. *P. putida* KT2440 has been used to produce different compounds such as aromatics, acids, alcohols, lactones, biopolymers, etc. [Nelson et al., 2002]. It is additionally employed in the synthesis of terpenoids, valued in the industry for their roles as flavor and fragrance additives [Weimer et al., 2020].

The SA pathway within the secondary metabolism of *P. putida* KT2440 also produces important metabolites. For example, muconic acid is the starting material for performance-advantaged bioproducts, and *P. putida* KT2440 has been engineered to synthesize muconate from both glucose and lignin [Bentley et al., 2020; Sonoki et al., 2018].

Protocatechuic acid (PCA) is another aromatic compound used in pharmaceutical, cosmetic, and food industries. Li et al. (2021) designed *P. putida* KT2440 for the high-level biosynthesis of PCA.

Since *P. putida* is a soil bacterium, it is exposed to harsh environmental conditions, which contributes to its metabolic and physiological resilience. It has the capability to quickly adjust to changing environmental factors, including elevated oxidative stress, temperature variations, sudden osmotic perturbations, and extreme pH [Nikel et al., 2018]. Moreover, the genomic data of *P. putida* is accessible, enabling targeted genetic modifications through the application of synthetic biology tools [Nikel et al., 2016]. Its rapid growth with minimal nutritional demands, capability to metabolize and degrade toxic compounds,

production of bio-based polymers, and modeling of genome-wide pathways have positioned it as an ideal chassis for biotechnological studies [Poblete-Castro et al., 2012].

2.3. *P. putida* KT2440 Metabolism

P. putida KT2440, renowned for its metabolic versatility, possesses the genetic capacity to catabolize a wide range of organic compounds, with its genome encoding enzymes for three distinct pathways of glucose metabolism: the Entner-Doudoroff (ED) pathway, the Embden-Meyerhof-Parnas (EMP) pathway, and the Pentose Phosphate Pathway (PPP).

Glucose is incorporated either through phosphorylation to glucose-6-phosphate (G6P) via glucokinase (Glk) or oxidation of the sugar to gluconate via glucose dehydrogenase (Gcd) or 2-ketogluconate via gluconate 2-dehydrogenase which further phosphorylated to 2-keto-6-phosphogluconate with 2-ketogluconate kinase (KguK) enzyme. 2-keto-6-phosphogluconate is further converted to 6-phosphogluconate (6PG) via 2-ketogluconate-6-P reductase (KguD). Also, gluconate can be directly converted to 6PG via gluconate kinase (GnuK) [Poblete-Castro et al., 2012].

Glycolysis is one of the most highly conserved biochemical pathways in living organisms, and it converts glucose into pyruvate by several reactions that provide energy and essential metabolites for cellular functions [Noor et al., 2010]. EMP, EDP, and PPP are the main pathways for glycolysis in bacteria [Conway, 1992]. While the early reactions of the ED and EMP pathways are distinct from each other; however, they merge in their later stages, both resulting in the production of pyruvate as a final metabolite.

The majority of glycolysis in *P. putida* KT2440 proceeds almost via the EDP, primarily due to the absence of 6-phosphofructo-1-kinase (Pfk), the enzyme responsible for converting fructose 6-phosphate (F6P) to fructose 1,6-bisphosphate (FBP). Glucose is converted to 6PG, with approximately 96% proceeding through the EDP via the action glucose-6-P 1 dehydrogenase enzyme encoded by the *zwf* gene. 6PG is subsequently converted into 2-keto-3-deoxy-6-phosphogluconate (KDPG) and then into pyruvate via the EDP through the actions of 6-phosphogluconate dehydratase (encoded by *edd*) and 2-keto-3-deoxy-6-phosphogluconate aldolase (encoded by *eda*), respectively. However, around 4% flux can enter into the PPP [Nikel et al., 2016].

In PPP, G6P is converted to the ribulose-5-P (Ri5P) via the action of 6-phosphogluconate dehydrogenase encoded by the gene *gnd*, producing NADPH and CO_2 in the process. Ri5P is converted into ribose-5-phosphate (R5P) and xylulose-5-phosphate (X5P). These intermediates can be used for the synthesis of nucleic acids. Key enzymes in this phase are ribose-5-phosphate isomerase (RpiA) and ribulose-5-phosphate epimerase (Rpe). Additionally, transketolase (TktA) and transaldolase (Tal) catalyze the conversion of PPP intermediates into F6P and glyceraldehyde-3-phosphate (G3P), which can re-enter glycolysis or be used in biosynthetic pathways. This pathway is particularly important for supplying reducing power in the form of NADPH, which is necessary for anabolic reactions and oxidative stress responses in *P. putida* KT2440. The flexibility of the PPP allows the bacterium to balance energy production, reducing power and biosynthetic precursor generation depending on the environmental conditions and available nutrients [Weimer et al., 2020].

G3P is sequentially converted into glycerate-3-phosphate (3PG) and then PEP through the enzymatic actions of glyceraldehyde-3-phosphate dehydrogenase (Gap), phosphoglycerate kinase (Pgk), phosphoglycerate mutase (Pgm), and enolase (Eno), respectively. Afterward, through the enzymatic actions of Pyk (PykA and PykF), PEP can be converted to pyruvate, which is directed into the Tricarboxylic Acid (TCA) cycle after being converted into acetyl-CoA by the enzyme pyruvate dehydrogenase. Also, PEP can be converted into oxaloacetate (OAA) via the enzyme PEP carboxylase (Ppc). Furthermore, PEP serves as a precursor for the SA pathway, where it combines with E4P, synthesized from PPP, to produce 3-deoxy-D-arabino-heptulosonate-7-phosphate (DAHP), the first intermediate in the synthesis of AAA: phenylalanine, tryptophan, and tyrosine (Figure 2.1) [Weimer et al., 2020].

The coordinated actions of enzymes from the EDP, PPP, and the incomplete EMP's route establish a cyclic metabolic structure in *P. putida* KT2440, identified as the EDEMP cycle (Figure 2.1). Specifically, a portion of the triose phosphate pool is recycled back to G6P through the EDEMP cycle. The EDEMP cycle in *P. putida* regulates NADPH production to enhance resilience against oxidative stress. Glucose 6-phosphate-1-dehydrogenase enzyme in the EDEMP cycle of strain *P. putida* KT2440 is directly coupled to the formation of NADPH production [Nikel et al., 2016].

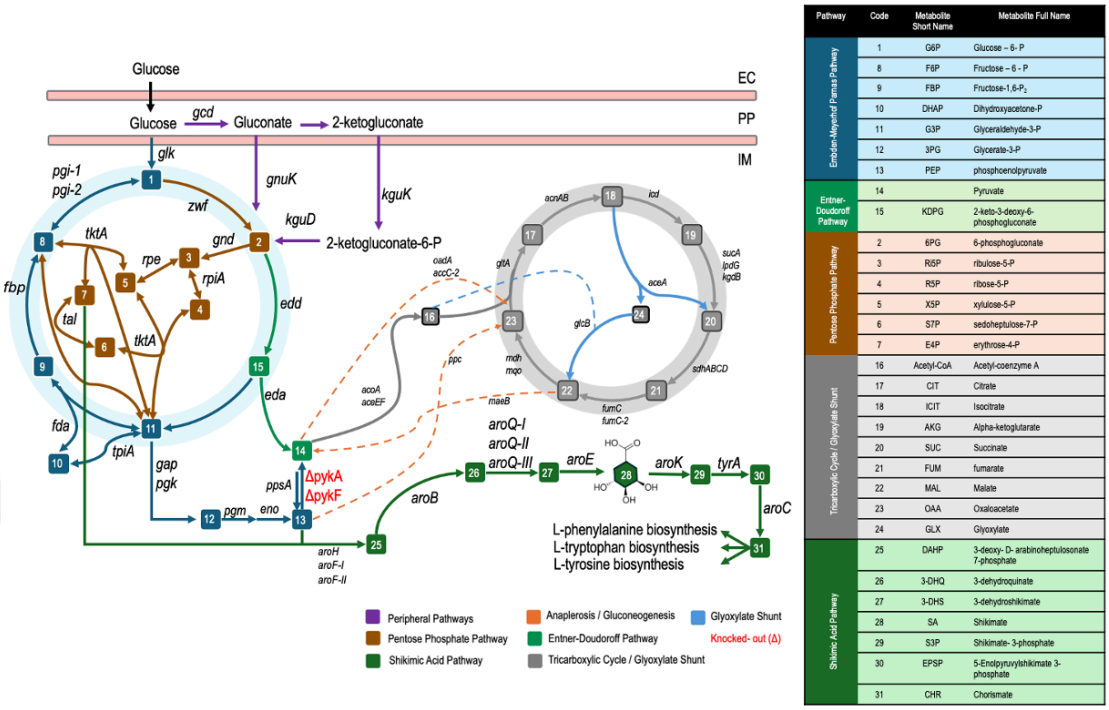

Pathway	Code	Metabolite Short Name	Metabolite Full Name
Embden-Meyerhof Parnas Pathway	1	G6P	Glucose – 6- P
	8	F6P	Fructose – 6 - P
	9	FBP	Fructose-1,6-P_2
	10	DHAP	Dihydroxyacetone-P
	11	G3P	Glyceraldehyde-3-P
	12	3PG	Glycerate-3-P
	13	PEP	phosphoenolpyruvate
Entner-Doudoroff Pathway	14		Pyruvate
	15	KDPG	2-keto-3-deoxy-6-phosphogluconate
Pentose Phosphate Pathway	2	6PG	6-phosphogluconate
	3	Ri5P	ribulose-5-P
	4	R5P	ribose-5-P
	5	X5P	xylulose-5-P
	6	S7P	sedoheptulose-7-P
	7	E4P	erythrose-4-P
Tricarboxylic Cycle / Glyoxylate Shunt	16	Acetyl-CoA	Acetyl-coenzyme A
	17	CIT	Citrate
	18	ICIT	Isocitrate
	19	AKG	Alpha-ketoglutarate
	20	SUC	Succinate
	21	FUM	fumarate
	22	MAL	Malate
	23	OAA	Oxalacetate
	24	GLX	Glyoxylate
Shikimic Acid Pathway	25	DAHP	3-deoxy- D- arabinoheptulosonate 7-phosphate
	26	3-DHQ	3-dehydroquinate
	27	3-DHS	3-dehydroshikimate
	28	SA	Shikimate
	29	S3P	Shikimate- 3-phosphate
	30	EPSP	5-Enolpyruvylshikimate 3-phosphate
	31	CHR	Chorismate

Figure 2.1: Central carbon metabolism and its connection to the shikimate pathway in *P. putida*. This diagram illustrates the glycolysis, EDP, EMPP, PPP, TCA cycle, along with pathways leading to the biosynthesis of AAA (L-phenylalanine, L-tryptophan, L-tyrosine) via the shikimate pathway. The deletion of genes encoding Pyk isoforms (Δ*pykA*, Δ*pykF*) is indicated in red.

Additionally, the products of this pathway provide essential carbon skeletons for the biosynthesis of amino acids, nucleotides, and other vital biomolecules, supporting growth and reproduction.

HexR is a key DNA-binding transcriptional regulator that represses the expression of glucose 6-phosphate dehydrogenase (*zwf*), 6-phosphogluconate dehydratase (*edd*), and glyceraldehyde 3-phosphate dehydrogenase (*gap*). Deletion of the glucose metabolism repressor hexR in *P. putida* KT2440 was implemented to enhance the intracellular availability of erythrose-4-phosphate (E4P) and NADPH, thereby increasing the titer of para-hydroxybenzoic acid (p-HBA) [Yu et al., 2016]. In addition, Bentley et al. (2020) reported that eliminating HexR repression increased the expression of suppressed genes in the PPP and EDP pathway in their metabolic engineering application on glucose metabolism of *P. putida* KT2440 to produce muconic acid. In this thesis, *P. putida* EM42Δ*hexR* strain [Akkaya, Ö unpublished] was used to improve SA production.

2.4. *P. putida* EM42

P. putida KT2440 is a host organism for heterologous gene expression; however, its efficiency is limited by the inefficient use of metabolic resources and genetic instability. Martínez-García et al. (2014) aimed to improve the capacity of *P. putida* for heterologous gene expression by deleting 300 genes across 11 chromosomal regions. The removal of the flagellar machinery and the proviral load enhances the physiological performance of the native strain.

Expressing foreign elements such as transposons and prophages, or other non-essential tasks into *P. putida* KT2440 can lead to genetic instability. When the bacterial genome was analyzed, 11 chromosomal regions (comprising 300 genes) with diverse cellular functions were identified (Figure 2.2). First, almost 2.6 % of the genome of *P. putida* KT2440 strain encodes prophages which are parasitic sequences. They increase the cells' susceptibility to DNA damage, and when activated, they trigger stochastic lysis within the bacterial population. Second, the locus encoding Tn7 transposon vectors may disrupt inserts aimed at the specific Tn7 integration site on the *P. putida* chromosome, which is commonly utilized for the stable integration of foreign DNA. One of the members of the Tn3 transposon family is the 15.7 kb Tn4652 which has activity only when the cells experience C starvation. *endA-1* and *endA-2* genes encoding two deoxyribonucleases I nick externally introduced plasmids and are also known to degrade plasmid DNA extracted from cells exhibiting DNase I activity. The presence of two such enzymes in *P. putida* makes it difficult to enter and gather plasmids. In addition, *hsdRMS* genes were removed because they typically defend the bacterium against foreign DNA. In addition, the complete flagellar rotor operon of *P. putida* KT2440 was deleted in the *P. putida* EM42 strain to increase the metabolic currency of ATP and NADPH. The absence of flagella

might not be significantly detrimental to the bacteria growing in shaken flasks or bioreactors [Martínez-García et al., 2014].

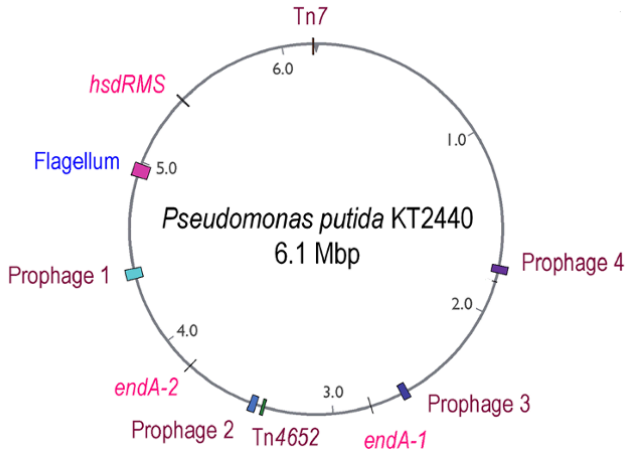

Figure 2.2: The positions of the eleven deleted gene regions in the genome of wild-type *P. putida* KT2440 leading to *P. putida* EM42 strain [Martínez-García et al., 2014].

2.5. Shikimic Acid (SA) Pathway

The shikimic acid (SA) pathway synthesizes essential vitamins and AAA like phenylalanine, tyrosine, and tryptophan in bacteria and several eukaryotes such as fungi, and plants. The SA pathway, named after its central intermediate, shikimic acid, consists of seven enzymatic steps. First, PEP and E4P are condensed into DAHP by the tyr-sensitive phospho-2-dehydro-3-deoxyheptonate aldolases encoded by *aroF-I*, *aroF-II* genes and 3-deoxy-7-phosphoheptulonate synthase enzyme encoded by *aroH*. DAHP is converted into 3-dehydroquinate (DHQ) by the enzyme dehydroquinate synthase encoded by the *aroB* gene. DHQ is transformed into 3-dehydroshikimic acid (DHS) catalyzed by 3-dehydroquinate dehydratase encoded by *aroQ*. Then, SA is synthesized by shikimate 5-dehydrogenase encoded by *aroE*. SA is transformed to shikimate-3-P (S3P) by the shikimate kinase encoded by *aroK*. S3P is converted to 5-enolpyruvylshikimate 3-phosphate (EPSP) and then chorismate (CHR) by 5-enolpyruvylshikimate-3-phosphate (EPSP) synthase encoded by *tyrA* and chorismate synthase encoded by *aroC* respectively.

Chorismate is recognized as an endpoint of the SA pathway and serves as a precursor for the synthesis of AAA like phenylalanine, tyrosine, and tryptophan, as well as other essential metabolites (Figure 2.3) [Li et al., 2020].

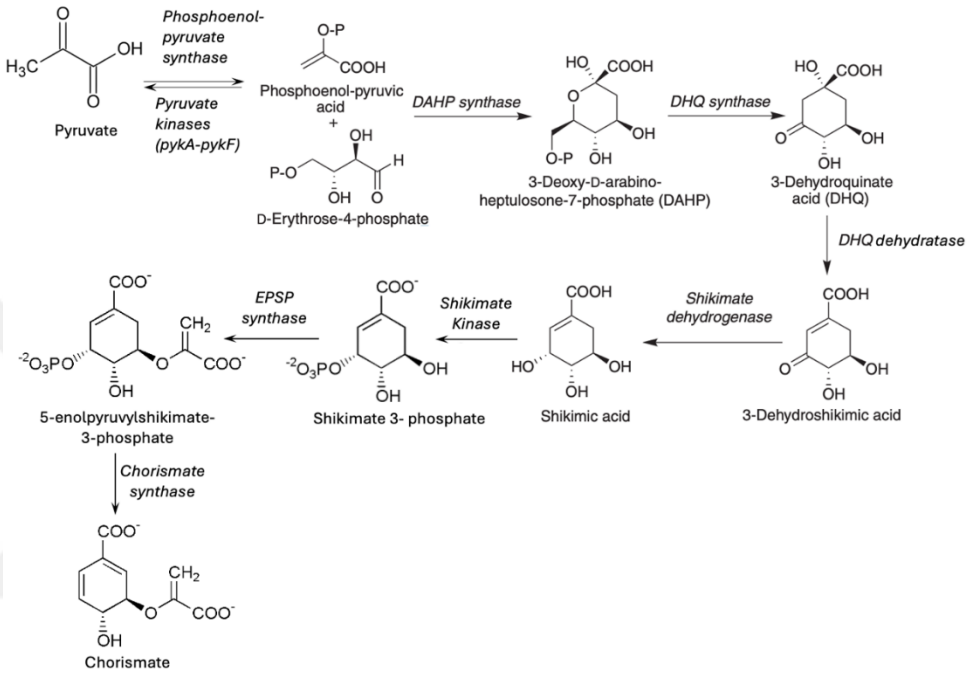

Figure 2.3: Molecular structures of the metabolites in the SA pathway [adapted from Alcántara et al., 2011].

The SA pathway is vital for the production of various secondary metabolites, including alkaloids, terpenoids, and aromatics such as vanillin, p-coumarate, phenol, and anthranilate [Weimer et al., 2020].

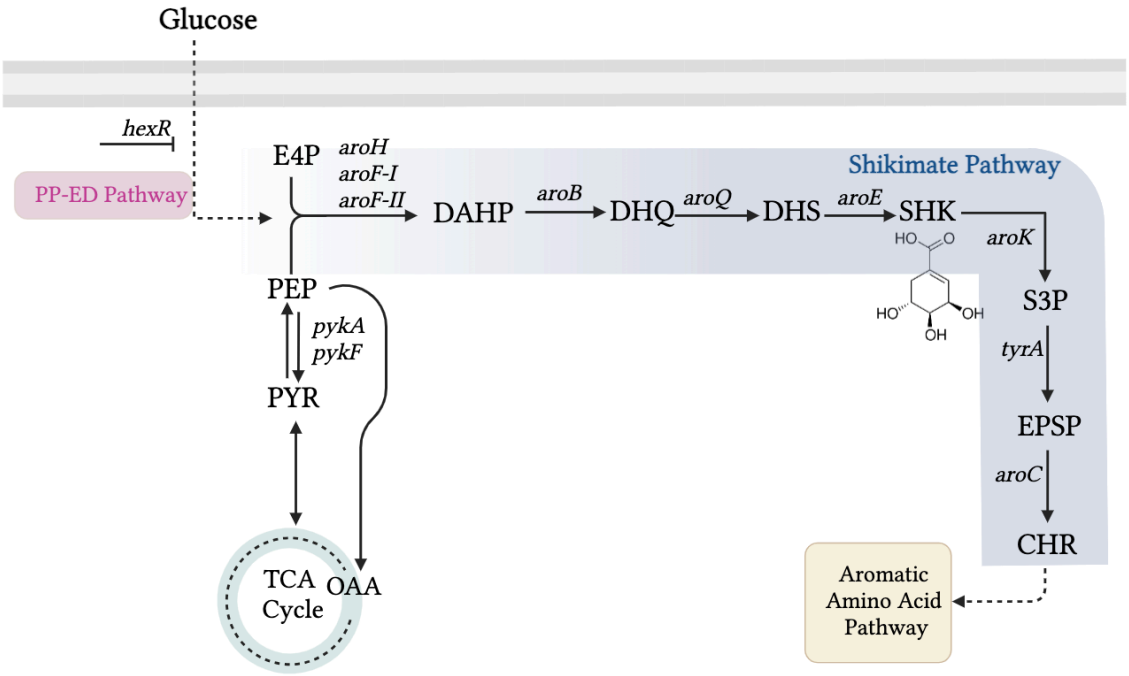

Figure 2.4: Metabolic pathways involved in the biosynthesis of SA in *P. putida*. The shikimate pathway converts glucose into chorismate, which is a precursor for the biosynthesis of AAA [adapted from Li et al., 2021].

SA pathway (Figure 2.4) is not found in animals; therefore, animals must retrieve AAA from their diets. Because of this metabolic difference, the enzymes of the SA pathway are selected as targets for herbicides and antimicrobial agents. This selectivity is crucial because it minimizes harm to animals, including humans. In addition, the SA pathway is responsible for the production of a variety of compounds valuable in the chemical, food, and pharma industries, including aromatics, non-aromatic acids, and shikimate pathway intermediates [Tzin et al., 2012].

For example, adipic acid is one of the most important dicarboxylic acids and serves as a monomer in the production of nylon 6,6. Environmental concerns can be reduced by targeting the biological production of adipic acid using engineered organisms [Babu et al., 2015]. Another metabolite is a naturally occurring organic acid -salicylic acid- which has great commercial value, especially in the cosmetic and pharmaceutical industries. It is used as the pharmaceutical precursor of aspirin and is also found in cosmetics in facial cleansers, lotions, and creams [Lin et al., 2014].

2.6. Pyruvate Kinase

2.6.1. The Reaction of Pyruvate Kinase

Pyruvate kinase (Pyk, E.C. 2.7.1.40) which is a key enzyme in glycolysis, conserved protein in both eukaryotes and prokaryotes [Hattori et al., 1995]. It is located at the connection point between the glycolysis and the TCA cycle therefore, it is crucial in cellular metabolism as it links with amino acid and lipid biosynthesis pathways.

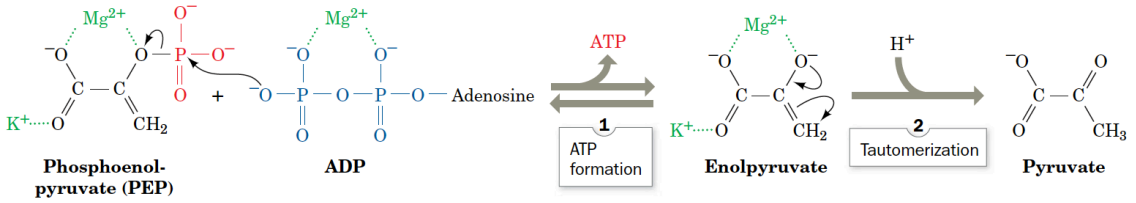

Figure 2.5: Conversion of PEP to pyruvate catalyzed by Pyk [adapted from Voet et al., 2012].

Pyk catalyzes the production of pyruvate from PEP in two steps (Figure 2.5). First, Pyk facilitates the transfer of the phosphoryl group from PEP to adenosine diphosphate (ADP), forming adenosine triphosphate (ATP) and enol pyruvate [Seeholzer et al., 1991]. Through the reaction, both monovalent (K^+) and divalent (Mg^{2+}) cations are required as cofactors to stabilize the negative charge [Voet et al., 2012]. The second step is the tautomerization of enolate to pyruvate spontaneously [Rose, 1970].

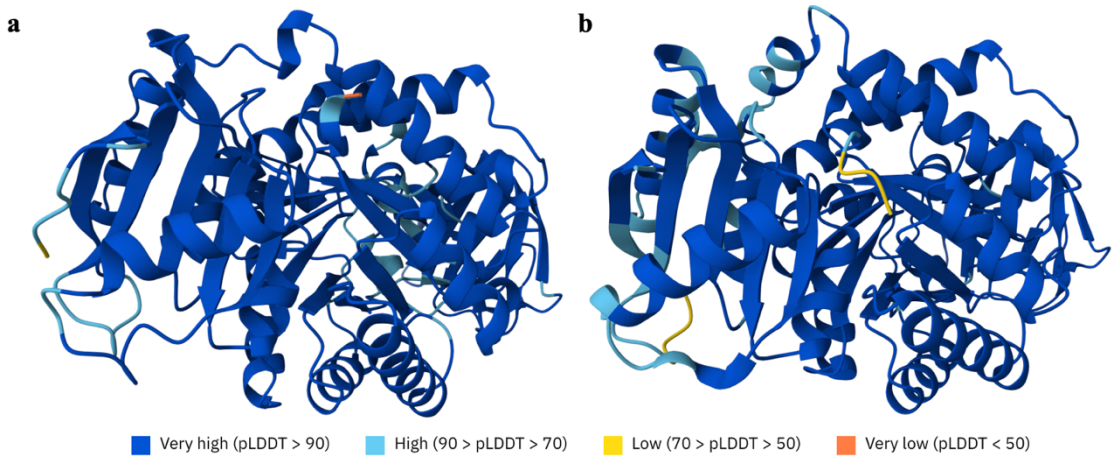

Figure 2.6: 3D structure of the a) PykA and b) PykF from *P. putida* KT2440 predicted by AlphaFold. The structure is color-coded based on pLDDT (predicted Local Distance Difference Test) confidence scores: Red (0-50, low confidence), yellow (50-70, intermediate confidence), light blue (70-90, high confidence), and dark blue (90-100, very high confidence). The model visualizes the predicted structural confidence across different regions of the protein. AlphaFold's prediction is based on homology to protein sequences available in the Protein Data Bank.

2.6.2. PykA and PykF in Different Bacteria

Most bacteria encode a single Pyk, although some species can have multiple Pyk isoforms. Bacterial species with two Pyks encode isoforms PykA (pyruvate kinase II) and PykF (pyruvate kinase I) [Munoz et al., 2003]. In the literature, Pyks isoforms in various organisms are studied extensively such as *E. coli* [Waygood et al., 1976], *P. aeruginosa* [Abdelhamid et al., 2019], *Yersinia species* [Hofmann et al., 2013], *Salmonella enterica* [Concepcion et al., 1987].

In addition, when comparing the primary amino acid sequences of PykA and PykF, the isoforms within the same organism exhibit less than 40 % similarity [Abdelhamid, 2019]. However, each isoform shows high similarity to other organisms of the same isoform (Table 2.1). It is proven that PykA contributes little to pyruvate kinase activity in *E. coli* metabolism [Siddique et al., 2004]. The effect of the *pykF* gene knockout was investigated by Siddique et al. (2004). They observed a decreased glucose uptake rate and lower flux ratios through lactate and acetate-forming pathways due to a decline in pyruvate availability.

Table 2.1: The percentage of amino acid sequence identity of Pyks among different bacteria [adapted from Abdelhamid et al., 2019].

	***P. putida* KT2440 PykA**	***P. aeruginosa* PykA**	***E. coli* PykA**	***S. typhimurium* PykA**	***Y. pestis* PykA**	***P. putida* KT2440 PykF**	***P. aeruginosa* PykF**	***E. coli* PykF**	***S. typhimurium* PykF**	***Y. pestis* PykF**	***M.tuberculosis* pyk**	***P. taiwanensis* pykA**	***P. taiwanensis* pykF**
***P. putida* KT2440 PykA**	100	83.2	56.9	57.1	56.3	38.0	37.6	37.5	37.7	38.5	39.4	98.4	37.3
***P. aeruginosa* PykA**		100	57.1	57.1	56.5	36.0	37.0	36.6	35.8	37.9	38.6	83.2	35.6
***E. coli* PykA**			100	98.5	90.6	38.0	39.2	36.7	36.5	36.9	38.5	56.9	38.2
***S. typhimurium* PykA**				100	90.6	37.7	39.2	36.7	36.3	37.1	38.5	57.1	38.0
***Y. pestis* PykA**					100	37.3	38.0	37.6	37.1	37.8	38.3	56.3	37.1
***P. putida* KT2440 PykF**						100	78.8	37.1	37.5	37.3	40.9	37.7	98.7
***P. aeruginosa* PykF**							100	36.9	37.3	37.3	40.9	37.6	79.6
***E. coli* PykF**								100	95.7	85.7	40.0	37.3	36.6
***S. typhimurium* PykF**									100	86.8	39.7	37.5	37.1
***Y. pestis* PykF**										100	40.0	38.3	36.9
***M.tuberculosis* pyk**											100	39.2	41.1
***P. taiwanensis* pykA**												100	37.1
***P. taiwanensis* pykF**													100

In the study conducted by Pan et al. (2006), when an inducible Pyk mutant (iPyk) similar to the *pyk* knockout mutant was created in *B. subtilis*, it was observed that this mutant led to reduced cell growth and an increase in the intracellular concentrations of PEP and G6P.

The effect of *pyk* gene knockout on the metabolism of *E. coli* in continuous culture was also investigated. It was found that in *pykF*$^{-}$ strain, flux through phosphoenolpyruvate carboxylase was up-regulated. Therefore, the concentrations of phosphoenolpyruvate, glucose-6-phosphate, and 6-phosphogluconate were increased [Al Zaid Siddiquee et al., 2004].

Chavadi et al. (2009) investigated the global effects of *Mycobacterium tuberculosis* Δ*pykA* mutant. Inactivation of the *pykA* gene in *M. tuberculosis* had effects on growth (slowed down) and resulted in dysgonic colony morphology. As a result, the levels of isocitrate dehydrogenase (*Icd2*) were improved, and isocitrate dehydrogenase (*Icl*) and phosphoenolpyruvate carboxylase (*PckA*) were decreased in the *pykA* knockout strain. In addition, enzymes involved in fatty acid and lipid biosynthesis declined, whereas those in β-oxidation were increased, indicating a shift toward using fatty acids for energy production.

2.7. I-SceI-based Method

One of the powerful tools to edit the genome of Pseudomonads is based on homologous recombination. With this method, genomic fragments can be deleted, altered, or inserted [Otto et al., 2020]. The I-SceI-based method developed by Martínez-García et al. (2012) is extensively used to remove undesired genomic segments. I-SceI is an endonuclease from the organism *Saccharomyces cerevisiae* that recognizes an 18-base pair DNA sequence and causes DSBs (double-strand break) by cutting I-SceI sites included in the plasmid [Köbbing, 2020]. The I-SceI enzyme is expressed intracellularly from the pSW-I plasmid. The *Pm* promoter of the pSW-I plasmid is induced by 3-methylbenzoate (3MB) [Martínez-García et al., 2012].

In this technique, up- and downstream fragments (target sites, TS1 and TS2) of the desired region are cloned into the suicide vector (*e.g.*, pEMG). The resulting plasmid is transferred into the target host. To be able to understand the transfer of the plasmid via homologous recombination, kanamycin-resistant clones are selected. In this procedure, I-SceI expressing plasmid (pSW-I) is introduced to the cell, controlled by 3MB inducible promoter system *XylS/Pm*, leading to DSB. Finally, gene-deleted or wild-type strains are

detected after repair occurs during the homologous recombination step via one of the flanking TS sites [Otto et al., 2020] (Figure 2.7).

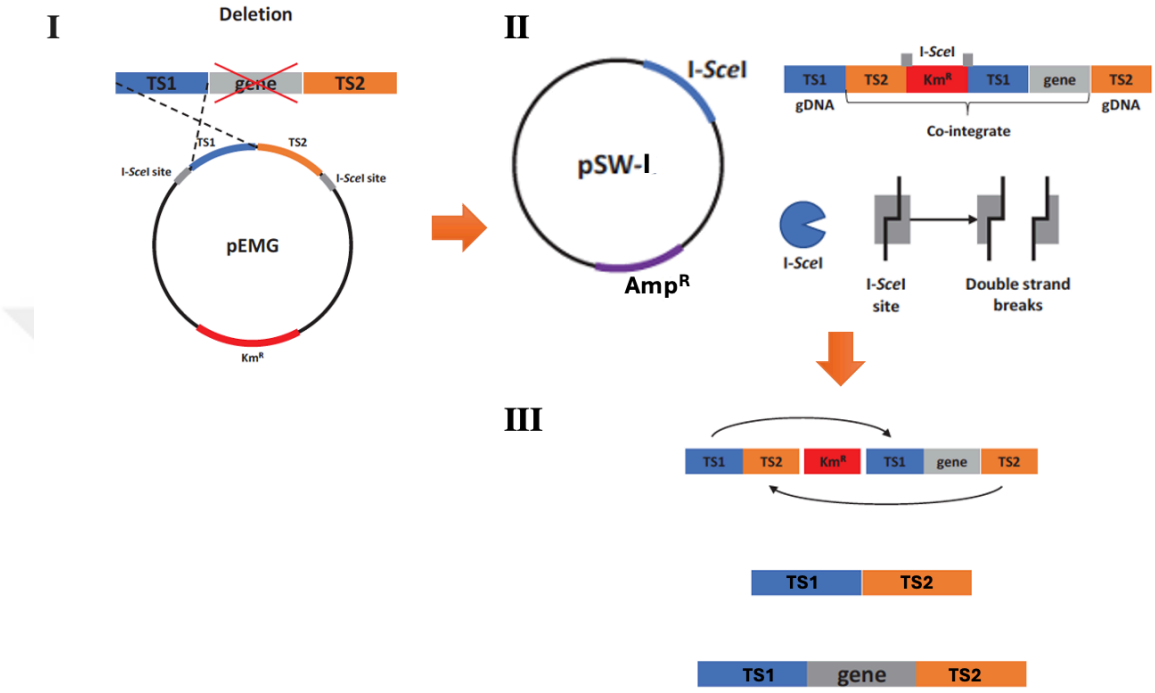

Figure 2.7: I-SceI-based homologous recombination method that renders the gene deletion [Köbbing, 2020]. (I) TS1-TS2 are cloned into the pEMG plasmid to create pEMG-TSs, showing the placement of the two I-SceI sites surrounding TS1-TS2. (II) The pEMG after genomic integration, I-SceI encoding pSW-I plasmid was induced by 3MB and introduced DSBs. (III) Different scenarios can occur. Deletion can either arise or wild-type situation can be restored.

3. MATERIALS AND METHODS

3.1. Materials

3.1.1. Bacterial Strains

Bacterial strains used in this work are listed in **Table 3.1**.

Table 3.1: Bacterial strains and plasmids used in this work.

	Description	References
***E. coli* strains**		
DH5α	Cloning host	[Hanahan et al., 1983]
DH5αλpir	Cloning host; λpir lysogen of strain DH5α	[Hanahan et al., 1980]
DH5αλpir-*pykA*	DH5αλpir containing pEMG-*pykA*, Km^R	This Study
DH5αλpir-*pykF*	DH5αλpir containing pEMG-*pykF*, Km^R	This Study
***P. putida* strains**		
KT2440	Wild-type strain; mt-2 derivative cured of the TOL plasmid pWW0	[Bagdasarian et al., 1981]
EM42	KT2440 derivative; Δprophage1 Δprophage4 Δprophage3 Δprophage2 ΔTn7 Δ*endA-1* Δ*endA-2* Δ*hsdRMS* Δflagellum ΔTn*4652*	[Martínez-García et al., 2014]
ΔX	EM42Δ*hexR*	[Akkaya, unpublished]
ΔXA	EM42Δ*hexR*Δ*pykA*	This Study
ΔXF	EM42Δ*hexR*Δ*pykF*	This Study
ΔXAF	EM42Δ*hexR*Δ*pykA*Δ*pykF*	This Study
Plasmids		
pRK600	Helper plasmid used for conjugation; *oriV* (ColE1), RK2(*mob*$^+$ *tra*$^+$); Cm^R	[Kessler et al., 1992]
pEMG	Plasmid used for deletions; *oriV*(R6K), *lacZα* fragment with two flanking I-SceI recognition sites; Km^R	[Martínez-García & de Lorenzo, 2011]
pSW-I	Helper plasmid used for deletions; *oriV* (RK2), *xylS*, Pm→I-SceI; Amp^R	[Wong et al., 2000]
pEMG-*pykA*	pEMG containing a fragment of *pykA*, Km^R	This Study

Table 3.1: Bacterial strains and plasmids used in this work (continue).

pEMG-*pykF*	pEMG containing a fragment of *pykF*, Km^R	This Study
Superscript "R" indicates resistance to the following antibiotics: Km kanamycin, Amp ampicillin, Cm chloramphenicol.		

3.1.2. Preparation and Concentration of Antibiotics

Kanamycin and ampicillin antibiotics are prepared in 100% dH_2O, and chloramphenicol is prepared in ethanol. They are filter-sterilized using 0.22 µm syringe filter units. Antibiotic stocks were aliquoted and stored at -20 °C. Concentrations of antibiotics used in this work are listed in **Table 3.2**.

Table 3.2: Concentration of antibiotics used in this work.

Antibiotics	**Stock (mg/ml)**	**Final concentration (µg/ml)**	
Strains		*P. putida*	*E. coli*
Kanamycin	50	50	50
Ampicillin	100	500	100
Chloramphenicol	30		30

3.1.3. Chemicals

Chemicals used in this work are listed in **Table 3.3**.

Table 3.3: Chemicals used in this work.

Chemical Name	**Company Name**	**Catalog Number**
LB Broth	Multicell	800060035
Agar	Biolife	05X036
Cetrimide Agar	Sigma Aldrich	VM1001184206
Ethanol	Sigma Aldrich	I1171483141
Acetonitrile	Sigma Aldrich	I1273130312

Table 3.3: Chemicals used in this work (continue).

KH_2PO_4 (Potassium dihydrogen phosphate)	ChemCruz	H1915
NaCI	Sigma Aldrich	K53298304134
NH_4CI (Ammonium chloride)	ChemCruz	I2815
D-Glucose	BIOFROXX	5D305CF3
Sucrose	CAISSON LABS	09192001
$MgSO_4$ (Magnesium sulfate)	AFG Bioscience	18855
Glycerol	BIOFROXX	60478016
$MgCl_2$ (Magnesium chloride)	AFG Bioscience	18740
PEG (Polyethylene glycol)	ALDRICH Chemistry	SLBG2838V
DMSO (Dimethyl sulfoxide)	MERCK	K38528043817
Tris Base	Sigma Aldrich	1003352123
Agarose	Invitrogen	0000230589
DNA loading dye	Hibrigen	0622-EC-2288
SYBR Safe DNA Gel Stain	Softec	0103000019
$Na_2HPO_4.2H_2O$ (Disodium hydrogen phosphate dihydrate)	ChemCruz	B0613

3.1.4. Devices

Devices used in this work are listed in **Table 3.4**.

Table 3.4: Devices used in this work.

Device Name	Device Model	Company Name
Precision Balance	ATX224	Shimadzu
pH Meter	HI 2211	Hanna Instruments
Incubator	ES-120	Nüve
Shaking Incubator	ZWYR-211C	Labwit
Spectrophotometer	UV-1800	Shimadzu
HPLC	SPD-20A, RID-10A modules	Shimadzu
Centrifuge	NF 1200R	Nüve
Rotary evaporator	Hei-VAP Precision	Heidolph

Table 3.4: Devices used in this work (continue).

Autoclave	CL-40L	Alp
Magnetic stirrer	MR3001	Heidolph
Laminar flow cabinet	MN 120	Nüve
Deep freezer (-20 ºC)	GSV33VW31N	Bosch
Refrigerator (+4 ºC)	NF48011	Vestel
Vortex	BV1000	Benchmark
Microwave oven	ME86V	Samsung
Nanodrop	NanoDrop Lite	Thermo Scientific
Thermal Cycler	T100™Thermal Cycle	BIO-RAD
Gel electrophoresis and power supply	Mini-Sub Cell GT and PowerPac™ Basic	BIO-RAD
Gel Imaging System	Universal Hood II	BIO-RAD
Electroporator	GenePulser Xcell	BIO-RAD
Ultrasonic Bath	UltraClean18	HydraUltrasonic
Heat Block	MaXtableH10	Daihan Scientific

3.2. Methods

3.2.1. Media, Solutions, and Buffers

3.2.1.1. Growth Media

Liquid, solid media, and solutions in this study are listed in **Table 3.5**. Prepared media were sterilized by autoclaving at 120 °C for 20 minutes.

Table 3.5: List of liquid, solid media, and solutions used in this study.

Media	**Per Litre**	**Preparation**
Liquid Media		
LB broth	10 g Casein Peptone 5 g Yeast Extract 5 g NaCl	LB broth was prepared by weighing the required amounts of ingredients and mixed with dH_2O in the desired volume. It was autoclaved as standard.

Table 3.5: List of liquid, solid media, and solutions used in this study (continue).

M9 minimal salts, 10x	85 g $Na_2HPO_4.2H_2O$ 30 g KH_2PO_4 5 g NaCI 10 g NH_4CI	Required amounts of ingredients were weighed, mixed with desired volume of Milli-Q water and autoclaved.
Solid Media		
LB agar	LB broth Agar	LB agar was prepared by adding 1.5% (w/v) agar to LB broth.
Cetrimide agar	45.3 g Cetrimide Agar 10 ml glycerol	45.3 g of Cetrimide agar was dissolved 1 liter of Milli-Q water. Media was heated in boiling water and agitated until completely dissolved. Required amount of glycerol was added and autoclaved.
Solution or Buffer		
TAE buffer, 50x	242 g Tris Base 57.1 ml Glacial Acetic Acid 37.2 g $Na_2EDTA.2H_2O$	The concentrations of the components were mixed in the required proportions and completed with Milli-Q water. It was adjusted to a pH of around 8.0-8.5. pH can be adjusted using HCl or NaOH.
$MgSO_4$ (1M)	120.4 g $MgSO_4$	120.4 g of $MgSO_4$ was dissolved in 1 liter of dH_2O and autoclaved.
Glucose (1M)	180,16 g glucose	180,16 g of glucose was dissolved in 1 liter of dH_2O and then filter-sterilized.
Sucrose (300mM)	102.69 g sucrose	102.69 g of sucrose was dissolved in 1 liter of dH_2O and then filter-sterilized.
$MgCl_2$ (1M)	95,2 g $MgCl_2$	95,2 g of $MgCl_2$ was dissolved in 1 liter of dH_2O and autoclaved.
TSS solution	100 g PEG 50 ml DMSO 50 ml $MgCl_2$ (1M)	The concentrations of the components were mixed in the required proportions and completed with LB broth. It was autoclaved as standard and stored at +4 ºC.
M9 minimal media	100 ml 10x M9 Minimal Salts 20 ml glucose (1M) 2.0 ml $MgSO_4$ (1M)	10x M9 minimal salts and $MgSO_4$ were prepared in water autoclaved as independently. Also, glucose was prepared in water and filter sterilized. The concentrations of the components were mixed in the required proportions and completed with sterilized dH_2O in a sterilized bottle.

3.2.2. DNA Techniques

3.2.2.1. Plasmid DNA Extraction

Plasmid DNA was isolated using the Macherey-Nagel (MN) Plasmid Miniprep Kit. After isolation, DNA was quantified using a NanoDrop.

3.2.2.2. Polymerase Chain Reaction (PCR)

To amplify the desired DNA region, PCR was carried out with the Q5® High-Fidelity DNA Polymerase (NEB, New England Biolabs). The PCR reaction mixture is listed in **Table 3.6**. The reaction was carried out as follows: 2 min at 98 °C; 30 cycles of 30 s at 98 °C, 30 s at 60 °C, and 30 s at 72 °C following the 10 min final incubation at 72 °C. The primers used in the study were manually designed, with their Tm values calculated using the Tm Calculator (https://tmcalculator.neb.com/) and synthesized by Oligomer.

Table 3.6: PCR reaction mix for amplifying the desired DNA region.

Ingredients	Volume (25 µl)
5X Q5 Reaction Buffer Solution	5 µl
10 mM dNTP	0.5 µl
10 µM 5' Primer	1.25 µl
10 µM 3' Primer	1.25 µl
DNA template	variable
Q5 DNA Polymerase	0.25 µl
ddH_2O	variable

3.2.2.3. Colony PCR

For the colony PCR, HOT FIREPol® Blend Master Mix RTL (12.5 mM $MgCl_2$) (Solis Biodyne) was used. The PCR reaction mixture is listed in **Table 3.7**. The steps of the PCR reaction can be found in **Table 3.8**.

Table 3.7: Components of the colony PCR reaction.

Ingredients	Volume (20 µl)
HOT FIREPol® Blend Master Mix Ready to Load (5x)	4 µl
Forward primer (10 µM)	0.5 µl
Reverse primer (10 µM)	0.5 µl
DNA template	variable
ddH_2O	Up to 20 µl

Table 3.8: Steps of the colony PCR reaction.

Step	Temperature (°C)	Time	Cycles
Initial activation	95 °C	12-15 min	1
Denaturation	95 °C	10-20 s	25- 30
Annealing	60-65 °C	30-0 s	
Elongation	72 °C	20 s–4 min	
Final Elongation	72 °C	5- 10 min	

Table 3.9: List of primers used in this work.

Primers	Sequence (5'-3')
P1	CGGAATTCGTTGCTGCAGTCAAGGCT
P2	GCTTCACTATAGGAGTCTGTGCTCCACTCGTTTCACAGCACAA
P3	GCACAGACTCCTATAGTGAAGC
P4	CGGGATCCGCAGCATAAAGCCCGAATC
P5	CGGAATTCAGCAACCTCAACGAAGAAGAC
P6	AACGCGCCCCCGGCAATCGATTGGGCAGTCTCAAGGATC
P7	GATTGCCGGGGGCGCGTT
P8	CGGGATCCAATATGGCCGACCAGGGCA
P9	CCCCATGCGCTCCATCAAGAAGA
P10	CGACTGGAAAGCGGGCAGTGAG
P11	GGACGCTTCGCTGAAAACTA
P12	AACGTCGTGACTGGGAAAAC
P13	ACAAGGCCGACATCAAACTG
P14	CGACGTGCAGGATCTTCATG
P15	GCCGAAGGCAAGGTGCAGT
P16	GGTTGGCGCTGGCGAGAAA

*:P1, *pykA*-TS1-F; P2, *pykA*-TS1-R; P3, *pykA*-TS2-F; P4, *pykA*-TS2-R; P5, *pykF*-TS1-F; P6, *pykF*-TS1-R; P7, *pykF*-TS2-F; P8, *pykF*-TS2-R; P9, pEMG-F; P10, pEMG-R; P11, pSW-F; P12, pSW-R; P13, *pykA*-internal-F; P14, *pykA*-internal-R; P15, *pykF*-internal-F; P16, *pykF*-internal-R

3.2.2.4. Agarose Gel Electrophoresis

1% agarose gel was prepared by dissolving 0.4 g agarose in 40 ml 1x TAE buffer using heating, adding 20,000x Syber Safe (Hibrigen) to achieve a final concentration of 0.75x. The PCR samples were loaded onto the gel in equal volumes and run using an electric current, generally 30 min at 100 volts. The gel was visualized using a Biorad imaging system.

3.2.2.5. Digestion of DNA

The pEMG plasmid was digested with the restriction enzymes *Eco*RI and *Bam*HI according to Martínez-García et al. (2012). The digestion mix contained 33 µl of TS1-TS2 PCR product, 4.5 µl of 10× buffer, 4.5 µl of BSA, 1.5 µl of *Eco*RI enzyme, and 1.5 µl of *Bam*HI enzyme. Finally, restriction enzymes were inactivated by heating.

3.2.2.6. DNA Isolation from Agarose Gel

1% agarose gel was prepared in 1x TAE buffer. 6x DNA loading dye was mixed with the DNA sample. The DNA sample was loaded onto the gel and run until the DNA was sufficiently separated. The gel was visualized under a UV transilluminator. DNA band corresponding to the target size was identified and excised from the gel using a scalpel. The excised gel was moved to the microcentrifuge tube which had already been weighed. The tube was weighed again to determine the excised gel weight. A Gel Extraction Kit (Macherey-Nagel) was used for the plasmid isolation from the agarose gel. Finally, the purified DNA concentration was determined using a Nanodrop and stored at -20 °C to proceed with downstream applications.

3.2.2.7. Ligation of DNA

TS1-TS2 digested fragments were ligated into the pEMG plasmid, and finally pEMG-TS plasmid was produced. The ligation mix ingredients were 6 µl digested TS1-TS2 PCR fragment, 3 µl of the pEMG plasmid, 10 µl of 2x buffer, and finally 1 µl T4 DNA ligase. The mixture was incubated overnight at 16 °C.

3.2.3. Preparation of Competent Cells

3.2.3.1. Preparation of Chemically Competent Cell

2 ml of LB medium was inoculated the night before with 20 µl of competent cell stock culture stored at -20 °C. 500 µl of overnight culture was inoculated to 50 ml fresh LB. The subculture was incubated at 37 °C with shaking at 170 rpm until the optical density at 600 nm (OD_{600}) reached 0.5. Cells were put on ice for 30 min and transferred to a falcon tube to centrifuge at 4000 rpm for 40 min at 4 °C. The cell pellet was resuspended in ice-cold Transformation and Storage Solution (TSS) at 1/10 volume of the culture. The resuspended cells were aliquoted into pre-chilled Eppendorf tubes, 200 µl each, and stored at -80 °C [Chung et al., 1989].

3.2.3.2. Preparation of Electrocompetent Cells

The protocol was adapted from Martínez-García et al. (2012). 20 ml of overnight culture were centrifuged at 4000 rpm, 25 °C for 20 min. The supernatant was carefully removed using a pipette, and the pellet was washed four times using sterile 300 mM sucrose. The pellet was resuspended 500 µl 300 mM sucrose for transformation and aliquoted with a volume of 100 µl each into 1.5 ml Eppendorf tubes.

3.2.4. Transformation

3.2.4.1. Chemical Transformation of *E. coli*

200 µl of competent cells were mixed with 5 µl of the ligation mixture and incubated for 30 min on ice. The cells were subsequently subjected to a heat shock at 42 °C for 45 s and immediately placed on ice for 5 min. 1 ml of LB was added, and the transformed cells were inoculated for 1-1.5 hours at 37 °C with shaking at 170 rpm. Finally, cells were centrifuged at 13.000 rpm for 1 min. The supernatant was carefully discarded, leaving a small amount, and the pellet was resuspended in the remaining supernatant. The entire

resuspension was plated onto an appropriate antibiotic-containing agar plate and incubated overnight at 37 °C.

3.2.4.2. Transformation of *P. putida* by Electroporation

The electrocompetent cells were mixed with 100 ng of plasmid DNA. The mixture was placed in the center of an electroporation cuvette, and transformation by electroporation was performed using a BIO-RAD GenePulser Xcell with the parameters 2500 V, 25 μF, 200 Ω, and cuvette size 2 mm. The cells were immediately resuspended 1 ml of LB and inoculated for 2 h at 30 °C on a rotating incubator. Finally, the cells were plated onto appropriate antibiotic-containing LB plates and incubated overnight at 30 °C [Martínez-García et al., 2012].

3.2.5. Gene sequencing

Gene sequencing was performed by Macrogen, with the samples being prepared according to the company's guidelines.

3.2.6. Conjugation

1 ml of overnight culture of donor cells: *E. coli* DH5α/pSW-I in LB-Amp at 37 °C, helper cells: *E. coli* HB101/pRK600 in LB-Cm at 37 °C, recipient cells: *P. putida* EM42 cells in LB at 30 °C were grown overnight. The cells were washed with 1 ml of 10 mM $MgSO_4$ and mixed in a 1:1:2 ratio into 10 mM $MgSO_4$. Then, the mixture was concentrated and laid onto a Millipore filter disk (0.45 μm pore-size, 13-mm diameter). The filters were incubated in the middle of the LB agar plate overnight at 30 °C (the optimum temperature for recipient cells). The filter was transferred to a 10 mM $MgSO_4$ and vortexed to resuspend the cells. Appropriate dilutions were plated onto a Cetrimide-Amp plate and incubated at 30 °C. After overnight incubation, colonies with blue-green and yellow-green colors were selected [Martínez-García et al., 2011].

3.2.7. Genome Editing

The I-SceI-based method developed by Martínez-García et al. (2011) is widely used for genomic deletions. *pykA* and *pykF* genes are deleted in *P. putida* ΔX strain using the I-SceI endonuclease system. First, upstream (TS1) and downstream (TS2) fragments of *pykA* and *pykF* genes are identified, and two pairs of primers that span the genes were designed. The next step was performed by splicing by overlap extensions (SOE)-PCR. For SOE-ing PCR, reverse complement primers sequence of TS1F to TS2R was added to the reaction for each gene. Also, enzyme restriction sites were included in the TS1-TS2 primers. *Eco*RI was added to the P1 and P5 primers, while *Bam*HI was added to the P4 and P8 primers. After SOEing PCR, the fragments were digested with *Eco*RI and *Bam*HI restriction enzymes and ligated into the already digested pEMG plasmid. pEMG-*pykA* and pEMG-*pykF* were produced. The pEMG-*pykA* and pEMG-*pykF* plasmids were delivered separately into the *E. coli* DH5αλpir by chemical transformation and plated onto LB-Km. Colony PCR was performed to confirm the presence of pEMG-*pykA* plasmid using P1-P4 primers and the presence of pEMG-*pykF* plasmid using P5-P8 primers (Table 3.9). Several positive colonies were screened by sequencing (Macrogen). Then, the pEMG-*pykA* and pEMG-*pykF* plasmids were delivered into the *P. putida* ΔX strain separately by electroporation and plated onto LB-Km. The colonies were streaked, and by using colony PCR, the cointegration process was checked. pSW-I plasmid was delivered separately by conjugation into the *P. putida* ΔX + pEMG-*pykA* and *P. putida* ΔX + pEMG-*pykF* strains and plated onto LB-Amp. The colony PCR was performed to check the presence of the plasmid using P11 and P12 primers (Table 3.9).

A colony harboring the pSW-I plasmid was induced in a 2 ml LB-Amp tube with 15 mM 3MB (induce the expression of the I-SceI) that recognizes I-SceI sites and introduces DSB. The induction time was between 12-16 hours. The induced cells, grown overnight, were diluted several times and plated onto an LB plate. Colonies were streaked in LB and LB-Km to check the loss of the plasmid. Km-sensitive colonies were selected. Deleted-clones and wild-type strains were compared by colony PCR. To confirm the deletion of the *pykA* gene, P13-P14 primers (Table 3.9) were used, while P15-P16 primers (Table 3.9) were employed to verify the deletion of the *pykF* gene.

To obtain *P. putida* ΔXAF, the pEMG-*pykF* plasmid, which was confirmed by sequencing, was introduced into the *P. putida* ΔXA strain via electroporation and plated onto LB-Km. Colony PCR was performed to confirm the presence of pEMG-*pykF* plasmid in the *P. putida* ΔXA strain using P5-P8 primers (Table 3.9). *P. putida* ΔXA + pEMG-*pykF* strain transformed with pSW-I plasmid, and the presence of the plasmid was controlled using P11-P12 primers (Table 3.9). After overnight induction with 3MB, colony PCR was performed with Km-sensitive colonies using both P13-P14 and P15-P16 primers (Table 3.9) to verify the deletion of both *pykA* and *pykF* genes.

3.2.8. Culture Growth

P. putida ΔX, ΔXA, ΔXF, ΔXAF bacterial strains were stored at -80 ºC. Shake flask experiments were conducted by inoculating seed cultures from glycerol stock into 10 ml of LB medium in a 50 ml Erlenmeyer flask, incubating overnight at 30 ºC at 170 rpm.

Then, overnight cultures are used to inoculate a second seed culture in 20 ml of LB medium in a 100 ml Erlenmeyer flask. OD_{600} is measured using a spectrophotometer and set to 0.1. The second seed cultures were incubated at 30 ºC at 170 rpm for 3-4 h depending on the strain until an OD_{600} was reached to approximately 1. Cultures were centrifuged at 4000 rpm for 20 minutes at 4 ºC, the pellets were resuspended in 10 ml of 1X M9 salts and were centrifuged at the same conditions. The pellets were resuspended in 4 ml of 1X M9 salts. The cells were inoculated in a 250 ml Erlenmeyer flask containing 50 ml M9 minimal media supplemented with 20 mM glucose with a starting OD_{600} of 0.1. The culture was grown at 30 ºC at 170 rpm.

Culture growth and pH were monitored by periodic measurement along with the collection of samples for the analysis of glucose consumption and metabolite production.

3.2.9. HPLC Analysis

3.2.9.1. Glucose Consumption Analysis

Glucose consumption was analyzed using the Shimadzu Series 10 Refractive Index Detector (RID). HPLC samples were collected by pipetting 1 ml of samples into 1.5 µL centrifuge tubes from Erlenmeyer flasks at the desired time points and placed into a centrifuge machine operated at 10,000 rpm for 15 minutes at 4°C. After centrifugation, the supernatants were filter-sterilized using a 0.22 µm syringe filter, transferred to the 2 ml HPLC vials, and ready for analysis.

Several different protocols were tested to identify the most suitable HPLC method for determining the amount of glucose consumed by bacteria. The methods used are listed in **Table 3.10**.

Table 3.10: Evaluated protocols for HPLC analysis of glucose.

Mobile Phase	Flow Rate (mL/min)	Column Temperature (°C)	Injection Volume (µL)
Acetonitrile: dH_2O (75:25)	0.6	25	20
Acetonitrile: dH_2O (75:25)	0.6	40	20
Acetonitrile: dH_2O (75:25)	1.0	25	20
Acetic Acid: dH2O (0.01:99.99)	0.6	25	20
Acetonitrile: dH_2O (80:20)	1.0	25	20

Separation was achieved using a InterSustain NH_2 column 5 µm, 4.6 x 150 mm using an isocratic flow at a flow rate of 0.6 mL/min. Acetonitrile/water (80/20) was used as the mobile phase for a total run time of 20 min. The oven temperature was set to 25 °C and the injection volume was 20 µL. Analytical standards were ranged from 0.2 to 5.4 g/L (1.25 mM to 30 mM) and a calibration curve was plotted.

3.2.9.2. Organic Acid Analysis

Samples taken at different times of the bacterial culture were centrifuged at 4000 rpm for 20 min at 4 ºC, supernatants were transferred to the rotary evaporation flask and separated from salts in the medium. Then, samples were filter-sterilized (0,22 μm) and transferred to the 2 ml HPLC vials for analysis.

For the detection of aromatics (shikimic acid, 3-dehydroshikimic acid), extracted and filtered samples were analyzed using a UV/VIS detector at a wavelength of 210 nm. Samples and standards were analyzed using Coregel 87H3 column, at a flow rate of 0.6 mL/min for 30 min at a temperature of 25 °C in the low-pressure gradient mode. A gradient of 0.01 acetic acid in water (A) and acetonitrile (B) was used with the injection volume of 20 μL. A calibration curve was plotted for concentration determination using pure shikimic acid (S5375, Sigma-Aldrich) and DHS (05616, Sigma-Aldrich) standards.

4. RESULTS

4.1. Bioinformatics

4.1.1. The operon of the *pykA* and *pykF* genes in *P. putida* KT2440

P. putida KT2440 encodes two pyruvate kinase genes: *pykA* (1455bp) and *pykF* or *pyk* (1416bp). Two genes are located over 3 m base pairs apart on the chromosome of *P. putida* KT2440. The analysis of the genomic position of *pykA* disclosed that it is located downstream of the hypothetical protein PP_1363 (BIOCYC ID) and upstream of *groL* which encodes a chaperonin GroEL protein. InterPro protein domain analysis revealed that PP_1363 known as tetratricopeptide repeat protein is recognized for facilitating protein-protein interactions [Abdelhamid, 2019].

The genetic cluster of *pykA* is more structured compared to *pykF* (Figure 4.1). The upstream of the *pykF* gene consists of PP_4296, *gcl*, *hyi*, *glxR*, and *ttuD* genes. InterPro results for hypothetical protein PP_4296 revealed that it is the GlcG-related carbohydrate metabolism protein. This family play roles in the biochemical pathways related to glucose or glucose-derived molecules. *Gcl* encodes glyoxylate carboligase, *hyi* encodes hydroxypyruvate isomerase, *glxR* encodes tartronate semialdehyde reductase, *ttuD* encodes hydroxypyruvate reductase proteins that catalyze a sequence of reactions involved in glyoxylate and dicarboxylate metabolism in *P. putida* KT2440. The downstream region of the *pykF* gene contains a hypothetical gene (PP_4302) whose functions are not associated with the glyoxylate pathway. BioCyc and KEGG databases are used to generate the genetic bioinformatics of the *pykA* and *pykF*.

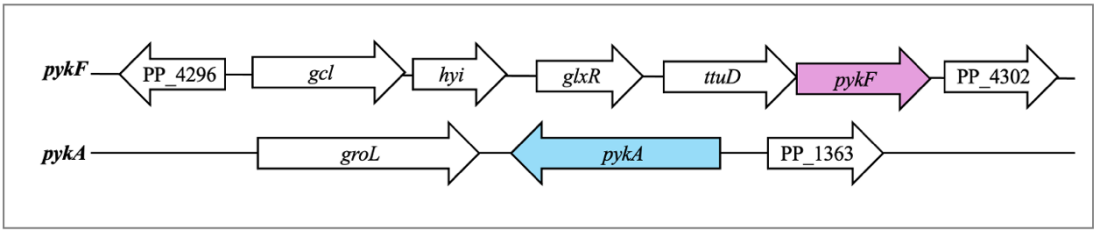

Figure 4.1: The genetic content of the pykA and pykF for wild-type *P. putida* KT2440.

4.1.2. Phylogenetic Analysis

The amino acid sequences of PykA and PykF from *P. putida* KT2440, *P. taiwanensis*, *P. aeruginosa*, *E. coli*, *S. Typhimurium*, *Y. pestis*, *M. tuberculosis* were aligned using the ClustalOmega tool. Then, the phylogenetic tree was generated using JalView from aligned sequences. In the phylogenetic analysis, the amino acid sequences of PykA and PykF were separated into two distinct groups. The results show that *P. putida* PykA and PykF are most closely related to *P. taiwanensis*, followed by *P. aeruginosa*.

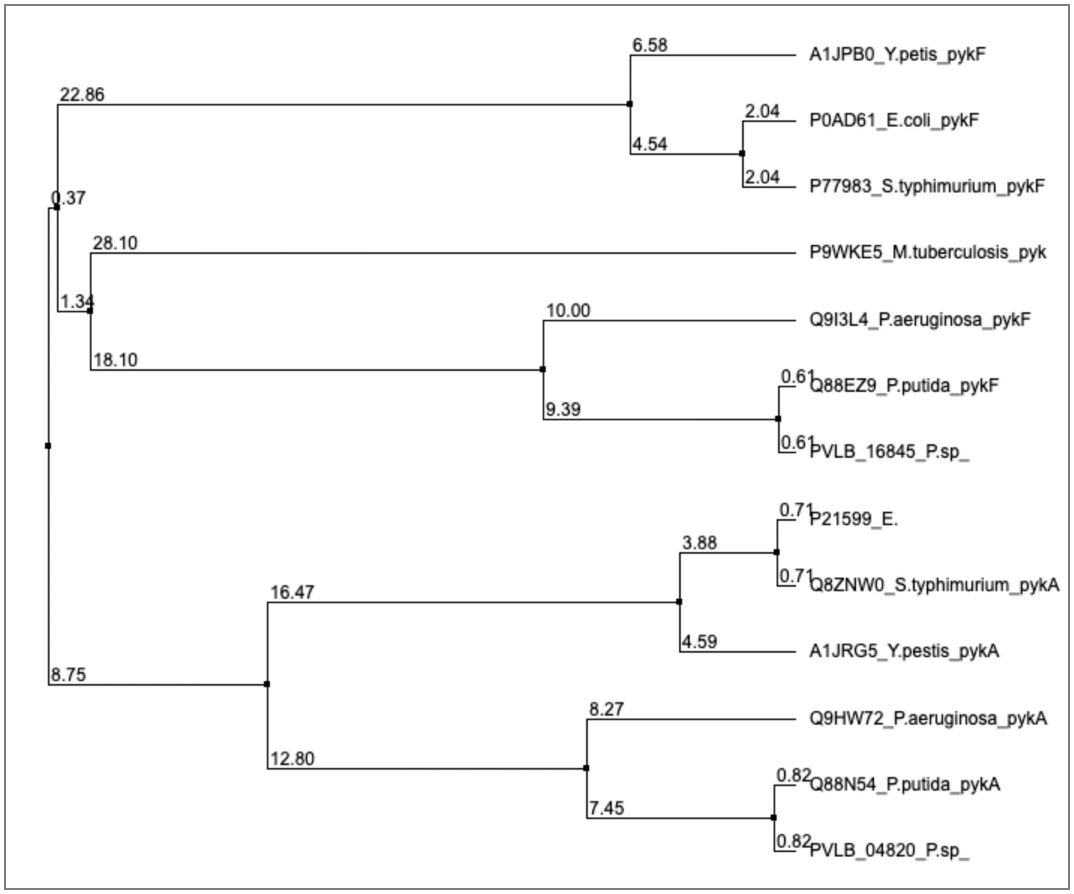

Figure 4.2: Phylogenetic tree of PykA and PykF aminoacid sequences in selected organisms. The first part is characterized by Uniprot ID following the organism and gene name. P. sp expresses *P. taiwanensis* as an organism. The alignment of the amino acid sequences was done by ClustalOmega, then JalView was used to calculate average distances from percentage sequence identity.

4.2. Deletion of Pyruvate Kinase Genes in *P. putida* EM42Δ*hexR* Strain

4.2.1. Deletion of *pykA* gene in *P. putida* EM42Δ*hexR* Strain

With I-SceI method, *pykA* gene was deleted in *P. putida* ΔX strain. Upstream (*pykA*-TSI) and downstream (*pykA*-TS2) sequences of the *pykA* gene were identified. P1, P2, P3, P4 primers of the *pykA* gene were designed and TS1 and TS2 fragments were amplified with PCR. Using the SOEing PCR method, the reverse complement sequence of P1 and P4 primers were added to the reaction. Moreover, *Eco*RI and *Bam*HI restriction sites were added to the P1 and P4 oligonucleotides, respectively. For optimization, different annealing temperatures were tested in the PCR protocol. After SOEing PCR (Figure 4.3), the *pykA*-TS1-TS2 PCR fragment was digested with *Eco*RI and *Bam*HI and isolated from agarose gel.

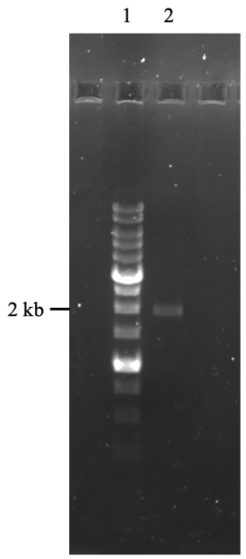

Figure 4.3: Agarose gel electrophoresis showing the SOEing PCR result. 1: marker (DNA Marker /1 kb, GenON) DNA ladder with bands at 10,000 bp, 8,000 bp, 6,000 bp, 5,000 bp, 4,000 bp, 3,000 bp, 2,500 bp, 2,000 bp, 1,500 bp, 1,000 bp, 750 bp, 500 bp, and 250 bp from top to bottom; 2: the result of SOEing PCR round, presenting the combined *pykA*-TS1-TS2 piece, 2 kb product.

TS1-TS2 digested PCR fragment was ligated into the pEMG vector (Figure 4.4.a) which was digested with the restriction enzymes *Eco*RI and *Bam*HI and purified from agarose gel (Figure 4.4.b) and the plasmid pEMG-*pykA* was generated.

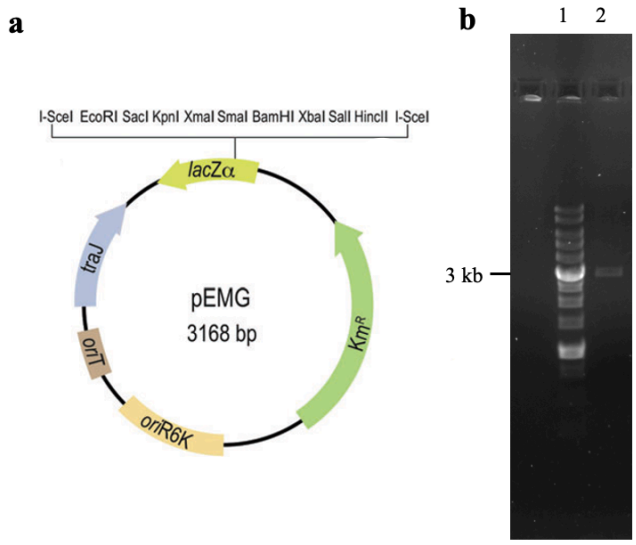

Figure 4.4: (a) Organization of the pEMG plasmid. It contains multiple cloning site (MSC) where homologous sequences can be inserted. The plasmid carries Km resistance gene. The plasmid can be used for conjugative mobilization (traJ, oriT), the origin of replication R6K which requires π protein supplied in trans [Martínez-García & de Lorenzo, 2011] (b) Agarose gel electrophoresis showing the digestion of pEMG plasmid with *Eco*RI-*Bam*HI restriction enzymes. 1: marker (DNA Marker /1 kb, GenON); 2: pEMG plasmid, ~3.2 kb product.

The plasmid pEMG-*pykA* was transformed into the *E. coli* DH5αλpir competent cells by chemical transformation and plated onto LB-Km. The colonies that have pEMG-*pykA* plasmid were selected and validated through colony PCR analysis. The 2 kb band was observed with P9-P10 primers in colonies 1 and 8 after colony PCR (Figure 4.5.). Then, the plasmid was sent for DNA sequencing to ensure the accuracy.

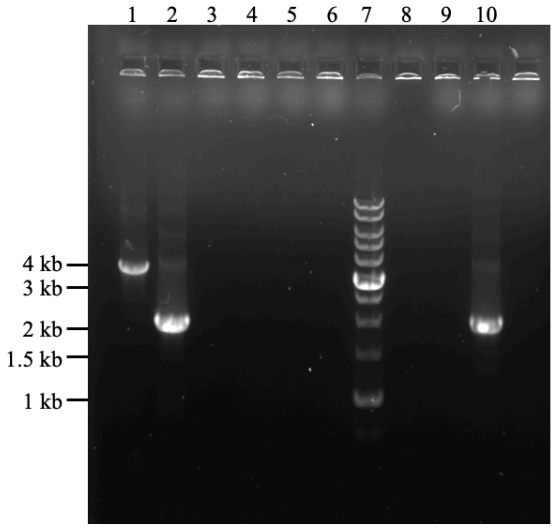

Figure 4.5: Agarose gel electrophoresis showing the results of colony PCR with P9-P10 primers for the verification of successful transformation of pEMG-*pykA* into *E. coli* DH5αλpir. 1: *P. putida* EM42 (positive control); 2-6: PCR products from colonies 1-5; 7: marker (DNA Marker /1 kb, GenON); 8-10: PCR products from colonies 6-8.

Once verified, 100 ng of pEMG-*pykA* plasmid was delivered to the *P. putida* ΔX strain by electroporation and plated on LB-Km Petri dish. The colonies were re-streaked and checked by colony PCR with P9-P10 primers (Table 3.9). Thus, the plasmid integration was confirmed (Figure 4.6). Colonies 2 (Figure 4.6.a) and 30 (Figure 4.6.b) were selected after electroporation.

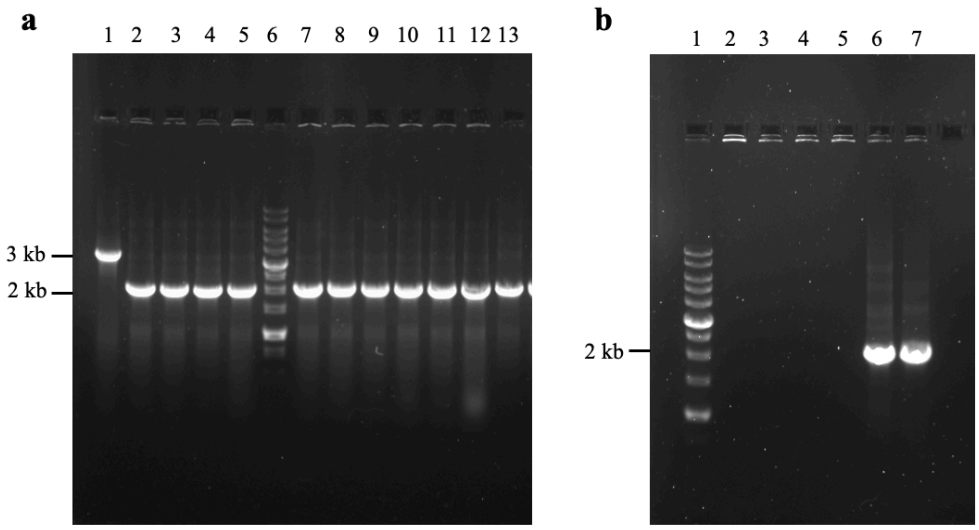

Figure 4.6: Agarose gel electrophoresis showing the results of colony PCR with P9-P10 primers for the verification of successful electroporation of pEMG-*pykA* plasmid into P. *putida* ΔX. (a) 1-5: PCR products from colonies 1-5; 6: marker (DNA Marker /1 kb, GenON); 7-12: PCR products from colonies 6-11; 13: pEMG-*pykA* plasmid (positive control). (b) 1: marker (DNA Marker /1 kb, GenON); 2-6: Colonies 12, 13, 14, 16, 30; 7: pEMG-*pykA* plasmid (positive control).

Conjugation was performed for both colonies 2 and 30 simultaneously to transfer the pSW-I plasmid (Figure 4.7). *P. putida* ΔX/pEMG-*pykA* strain as a recipient, *E. coli* DH5α/pSW-I as the donor cell, and *E. coli* HB101/pRK600 as a helper strain are used in conjugation.

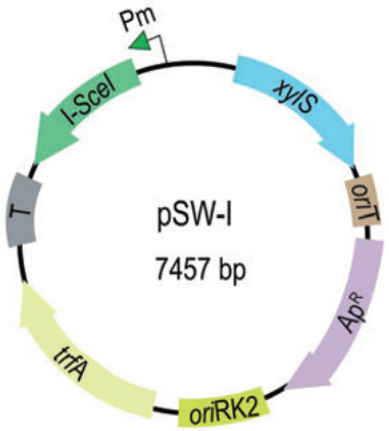

Figure 4.7: Organization of the pSW-I plasmid described by Wong et al. (2000) *Pm* promoter, regulated by *XylS*, is induced by 3MB to express the I-SceI nuclease conditionally [Blatny et al., 1997]. A transcriptional terminator (T), oriK2/trfA origin of replication, oriT conjugation transfer origin, and Amp^R resistance gene are located on the plasmid [Martínez-García & de Lorenzo, 2011].

Then, the cells were plated into Cetrimide-Amp, and the green colonies were re-streaked (Figure 4.8.a). Colony PCR was performed with the green colonies using the P11-P12 primers (Tablo 3.9), and the presence of a 520 bp band was confirmed (Figure 4.8.b). Thus, the presence of the pSW-I plasmid within the cells was validated. Also, P9-P10 primers were used at the same time, and the presence of the 2 kb band was confirmed (Figure 4.8.b).

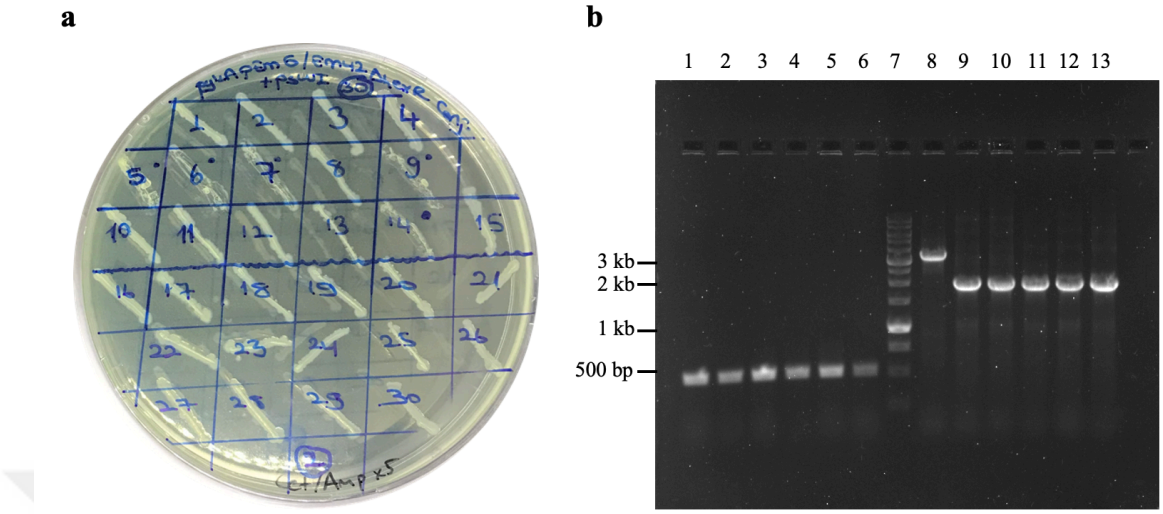

Figure 4.8: (a) Conjugation of the pSW-I plasmid to *P. putida* ΔX/pEMG-*pykA* was confirmed by re-streaked bacterial colonies grown on Cetrimide-Amp (b) Agarose gel electrophoresis showing the results of colony PCR with selected colonies from (a). P11-P12 and P9-P10 primers for the verification of successful conjugation of pSW-I plasmid into *P. putida* ΔX/pEMG-*pykA*. 1-5: PCR product from 5, 6, 7, 9, 14 colonies with P11-P12 primers; 6: *E. coli* DH5α/pSW-I with P11-P12 primers (positive control); 7: marker (DNA Marker /1 kb, GenON); 8-12: PCR product from 5, 6, 7, 9, 14 colonies with P9-P10 primers; 13: pEMG-*pykA* plasmid with P9-P10 primers (positive control).

Colonies 6 and 9 obtained from conjugation were selected, and the promoter system was induced overnight with 15 mM 3MB. This aimed to remove the target gene expressing the I-SceI nuclease. After several dilutions, the induced cells were spread on LB agar plates. The colonies were streaked simultaneously onto LB and LB-Km plates. While no Km-sensitive colonies were observed from the induction of colony 6 (Figure 4.9.a, b), Km-sensitive clones were identified from the induction of colony 9 (Figure 4.9.c, d). Finally, the deletion of the *pykA* gene was confirmed by performing colony PCR using P13-P14 primers on the Km-sensitive colonies. No specific bands were observed in any of the samples, and the *P. putida* ΔXA strain was successfully obtained (Figure 4.10).

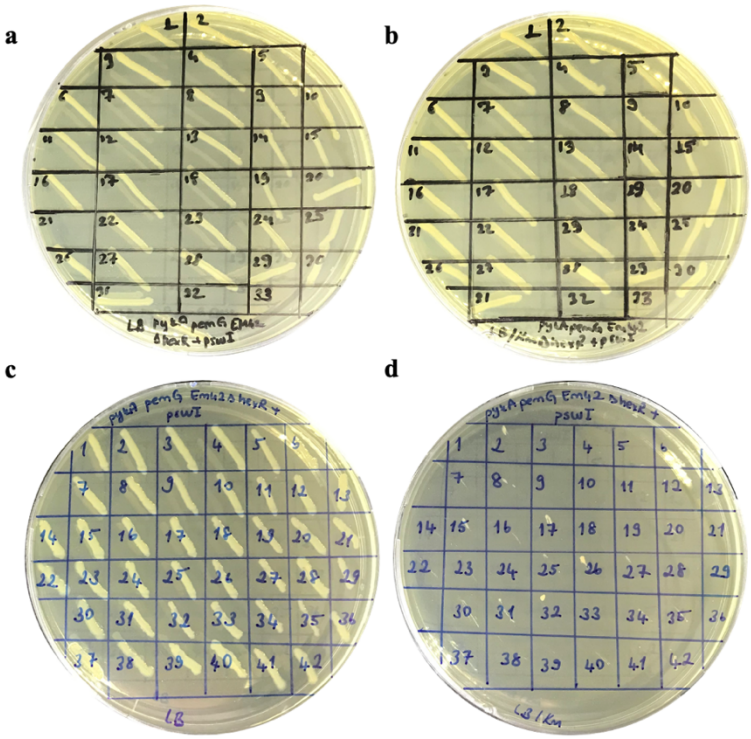

Figure 4.9: Re-streaked the colonies onto LB and LB-Km plates after induction (a) Re-streaking of the colony 6 on an LB agar after induction. (b) Re-streaking of the colony 6 on an LB-Km plate after induction. (c) Re-streaking of the colony 9 on an LB agar after induction. (d) Re-streaking of the colony 9 on an LB-Km plate after induction.

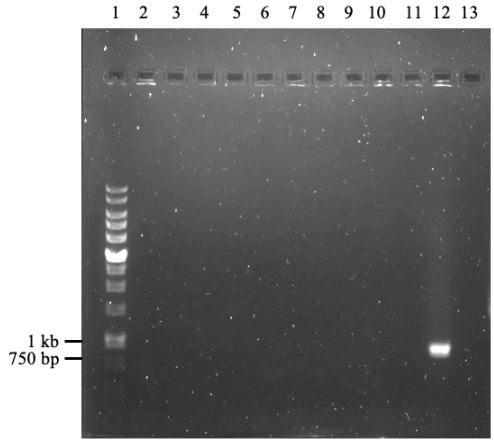

Figure 4.10: Agarose gel electrophoresis showing the results of colony PCR with P13-P14 primers for the verification of successful *pykA* gene deletion in *P. putida* XΔ strain. 1: marker (DNA Marker /1 kb, GenON); 2-11: 1-10 colonies; 12: *P. putida* EM42 (positive control); 13: negative control (no DNA template).

4.2.2. Deletion of *pykF* gene from *P. putida* EM42Δ*hexR* Strain

Upstream (*pykF*-TS1) and downstream (*pykF*-TS2) of the *pykF* gene region were defined. Two pairs of primers (P5, P6, P7, P8) that span each 750 bp of the *pykF* gene were designed. For SOEing PCR, reverse complement primer sequences of P5 and P8 were used in the PCR reaction (Figure 4.11). In addition, the *Eco*RI restriction site was added to the P5 primer, and *Bam*HI was added to the P8 oligonucleotide. For the PCR reaction, different concentrations of Mg^{2+} and annealing temperatures were tried for optimization. *pykF*-TS1-TS2 PCR fragment was digested with *Eco*RI and *Bam*HI and isolated from the agarose gel.

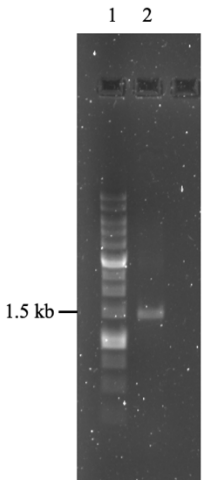

Figure 4.11: Agarose gel electrophoresis showing the SOEing PCR result. 1: marker (DNA Marker /1kb, GenON); 2: the result of SOEing PCR round, presenting the combined *pykF*-TS1-TS2 piece, 1500 bp product.

The *pykF* gene was cloned into the pEMG plasmid, which serves as a suicide vector for homologous recombination. pEMG plasmid was digested with *Eco*RI and *Bam*HI restriction enzymes and purified from the agarose gel. Digested TS1-TS2 PCR fragments were also isolated from agarose gel and ligated into the pEMG plasmid. Then, the recombinant *pykF*-pEMG plasmid was transformed into *E. coli* DH5αλpir competent cells and were plated onto LB-Km. By colony PCR with P5 and P8 primers, positive colonies were selected. The 1.5 kb band was obtained from colony PCR using colonies 2 and 3 as

templates (Figure 4.12), and isolated pEMG-*pykF* plasmids from these colonies were sent for sequencing.

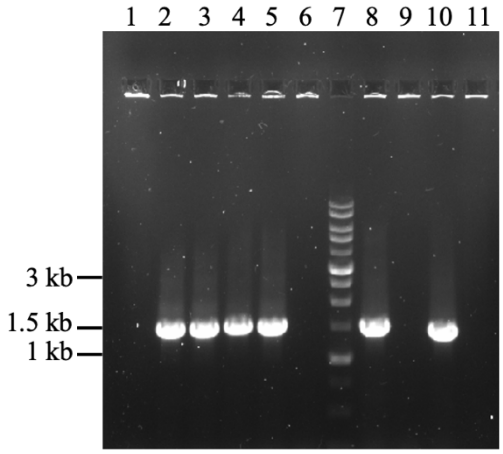

Figure 4.12: Agarose gel electrophoresis showing the results of colony PCR with P5 and P8 primers for the verification of successful transformation of pEMG-*pykF* into *E. coli* DH5αλpir. 1-6: PCR products from colonies 1-6; 7: marker (DNA Marker /1 kb, GenON); 8-10: PCR products from colonies 7-9; 11: *P. putida* EM42 (positive control).

Once verified, 100 ng of pEMG-*pykF* plasmid was delivered to the *P. putida* ΔX strain by electroporation and plated onto LB/Km. The colonies were re-streaked and checked by colony PCR with P9 and P10 primers, and *P. putida* ΔX/pEMG-*pykF* strain was verified (Figure 4.13.a). Colonies 5 and 8 were selected, and then colony PCR was performed again on these colonies with P5 and P8 primers (Figure 4.13.b). For colony 5, a 2 kb band was observed with P9 and P10 primers, and a 1.5 kb band was observed with P5 and P8 primers. Therefore, this colony was selected as the recipient cell for conjugation.

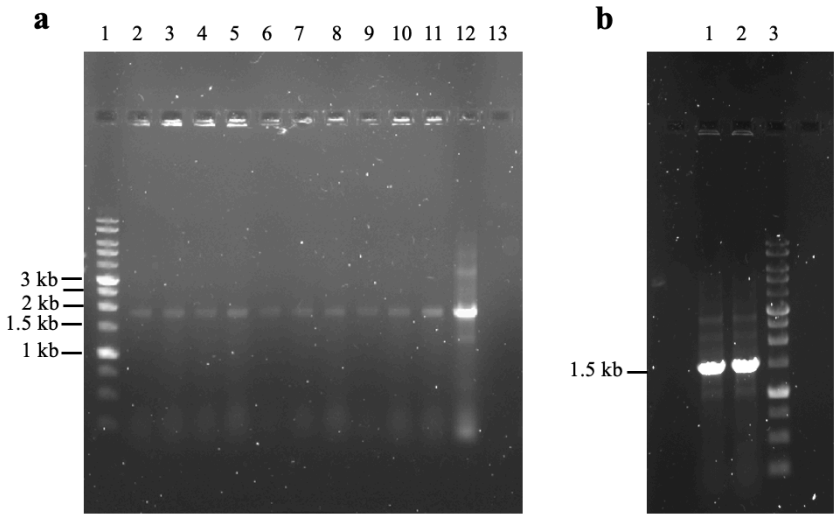

Figure 4.13: Image of an %1 agarose gel showing colony PCR results after 100 ng electroporation of pEMG-*pykF* plasmid into *P. putida* ΔX. (a) colony PCR with P9 and P10 primers 1: marker (1kb DNA Marker, Ecotech) DNA ladder with bands at 25,000 bp, 10,000 bp, 8,000 bp, 6,000 bp, 5,000 bp, 4,000 bp, 3,000 bp, 2,500 bp, 2,000 bp, 1,500 bp, 1,000 bp, 750 bp, 500 bp, and 250 bp from top to bottom; 2-11: PCR products from colonies 1-10; 12: pEMG-*pykF* plasmid (positive control); 13: negative control (no DNA template). (b) colony PCR with P5 and P8 primers. 1: colony 5 checked with P5 and P8 primers; 2: colony 8 checked with P5 and P8 primers; 3: Marker (1kb DNA Marker, Ecotech).

In addition, 200 ng pEMG-*pykF* plasmid was delivered to the *P. putida* ΔX strain by electroporation and plated onto LB-Km. The colonies were re-streaked, and by colony PCR with P9 and P10 primers (Figure 4.14.a) and P5 and P8 primers (Figure 4.14.b), *P. putida* ΔX/pEMG-*pykF* strain was verified simultaneously. For colony 19, a 2 kb band was observed with P9 and P10 primers, and a 1.5 kb band was observed with P5 and P8 primers, and this colony was selected as another recipient cell for conjugation.

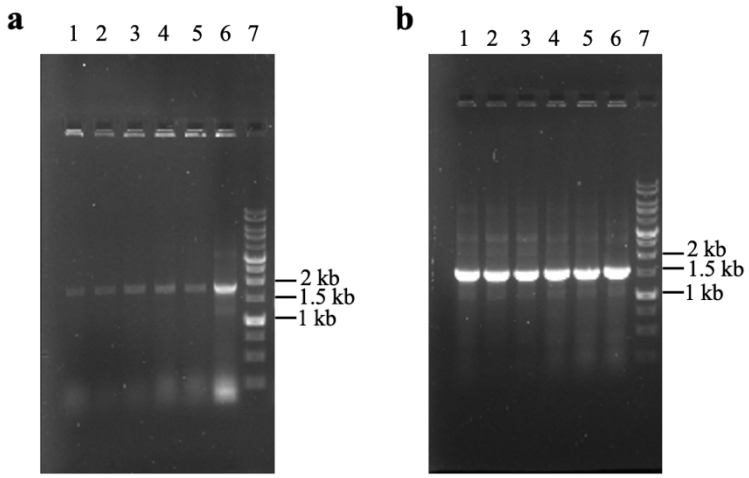

Figure 4.14: Image of an %1 agarose gel showing colony PCR results after 200 ng electroporation of pEMG-*pykF* plasmid into *P. putida* ΔX. (a) colony PCR with P9 and P10 primers. 1-5: 18-22 colonies; 6: pEMG-*pykF* plasmid (positive control); 7: marker (1kb DNA Marker, Ecotech). (b) colony PCR with P5 and P8 primers. 1-5: 18-22 colonies; 6: pEMG-*pykF* plasmid (positive control); 7: marker (1kb DNA Marker, Ecotech).

P. putida ΔX/pEMG-*pykF* strain was used as the recipient cell, and *E. coli* DH5α/pSW-I was used as the donor cell to transfer the pSW-I plasmid via conjugation. After conjugation, the cells were plated into Cetrimide-Amp, and the green colonies were re-streaked (Figure 4.15). P11 and P12 primers were used to check the presence of the plasmid by colony PCR, and the presence of a 520 bp band indicated the presence of pSW-I. Colony PCR was performed using P9 and P10 (Figure 4.16.a) and P11 and P12 (Figure 4.16.b) primers with colonies 4, 5 and 6, 8. These colonies (4 and 5) were selected for further analysis.

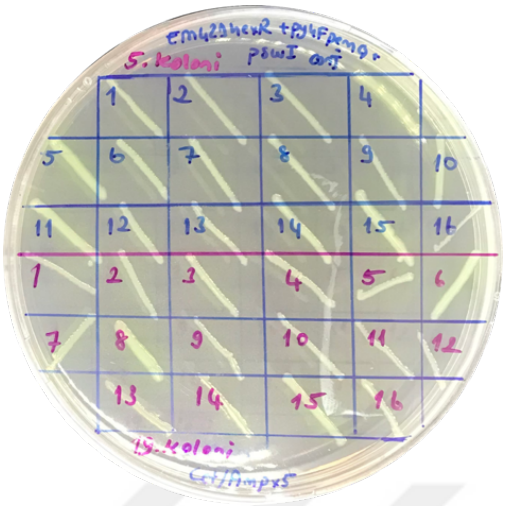

Figure 4.15: Re-streaked bacterial colonies grown on Cetrimide-Amp, following conjugation of pSW-I plasmid into *P. putida* ΔX/pEMG-*pykF*.

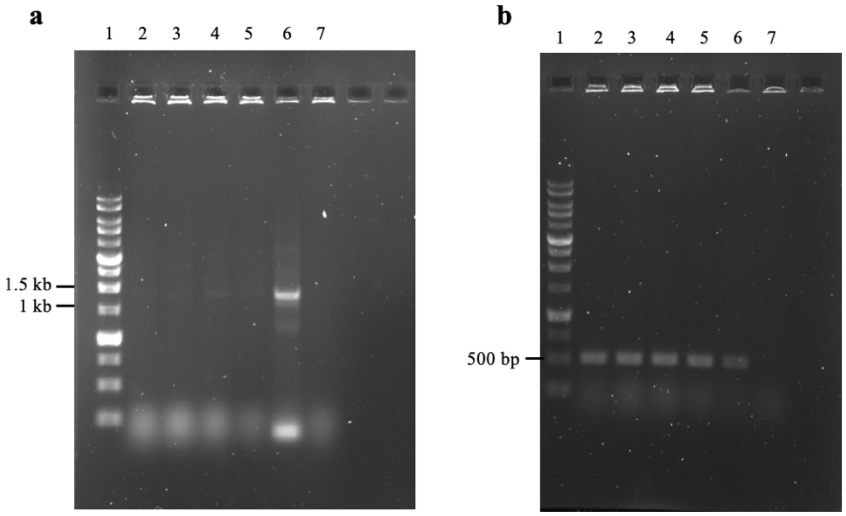

Figure 4.16: Image of an %1 agarose gel showing colony PCR results with P9-P10 and P11-P12 primers for the verification of conjugation pSW-I plasmid into *P. putida* ΔX/pEMG-*pykF*. (a) colony PCR with P9-P10 primers. 1: marker (1kb DNA Marker, Ecotech); 2, 3: colonies 4 and 5 from the conjugation of colony 5 as recipient cell; 4, 5: colonies 6 and 8 from the conjugation of colony 19 as recipient cell; 6: pEMG-*pykF* plasmid (positive control); 7: *P. putida* EM42. (b) colony PCR with P11-P12 primers. 1: marker (1kb DNA Marker, Ecotech); 2, 3: colonies 4 and 5 from the conjugation of colony 5 as recipient cell; 4, 5: colonies 6 and 8 from the conjugation of colony 19 as recipient cell; 6: *E. coli* DH5α/pSW-I (positive control); 7: *P. putida* EM42.

The promoter system was induced overnight with 15 mM 3MB to generate a DSB at the I-SceI recognition site, promoting the removal of the target gene through homologous recombination. Few dilutions were plated into LB agar, and colonies were re-streaked on LB and LB-Km plates. No Km-sensitive colonies were obtained.

Furthermore, colony PCR was performed again on colonies 1, 2, 3, 6, 7. The PCR was carried out using P9-P10 (Figure 4.17.a), P11-P12 (Figure 4.17.b) and P5-P8 (Figure 4.17.b) primers. Colonies 2 and 7 were selected for further analysis.

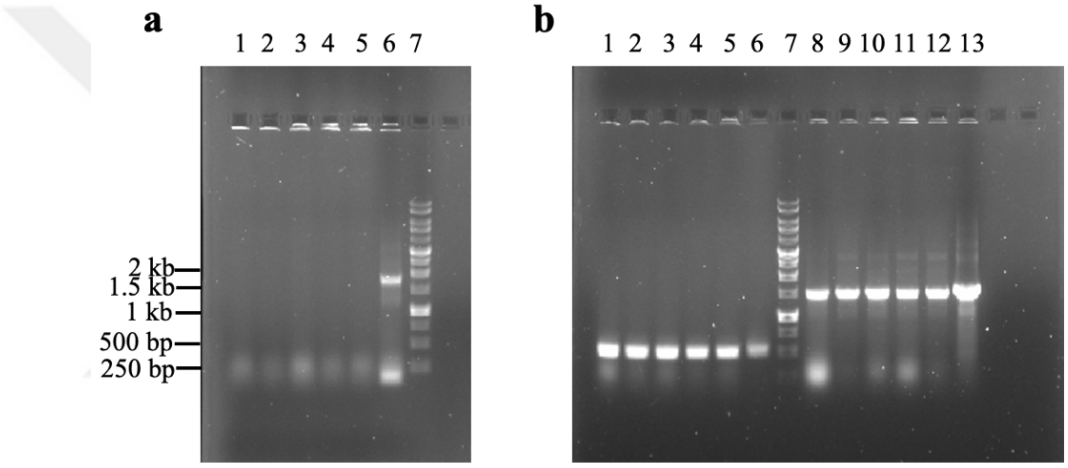

Figure 4.17: Image of an %1 agarose gel showing colony PCR results with P9-P10, P11-P12, and P5-P8 primers for the verification of conjugation pSW-I plasmid into *P. putida* ΔX/pEMG-*pykF*. (a) colony PCR with P9-P10 primers. 1-5: 1, 2, 3, 6, 7 colonies from the conjugation of colony 5 as recipient cell; 6: pEMG-*pykF* plasmid (positive control); 7: marker (1kb DNA Marker, Ecotech). (b) Colony PCR with P11-P12 and P5-P8 primers. 1-5: PCR result of 1, 2, 3, 6, 7 colonies from the conjugation of the colony 5 as a recipient cell with P11-P12 primers; 6: *E. coli* DH5α/pSW-I (positive control) with P11-P12 primers; 7: marker (1kb DNA Marker, Ecotech); 8-12: PCR result of 1, 2, 3, 6, 7 colonies from the conjugation of the colony 5 as a recipient cell with P5-P8 primers; 13: pEMG-*pykF* plasmid (positive control) with P5-P8 primers.

After conjugation, colonies 2 and 7 were induced overnight. Few dilutions were plated into LB agar, and colonies were re-streaked in LB and LB-Km (Figure 4.18). As a result of the overnight induction of colony 2, colonies 17 and 64 were resistant to the Km (Figure 4.18.b). After the induction of colony 7, only colony 45 was found as resistant to Km (Figure 4.18.d).

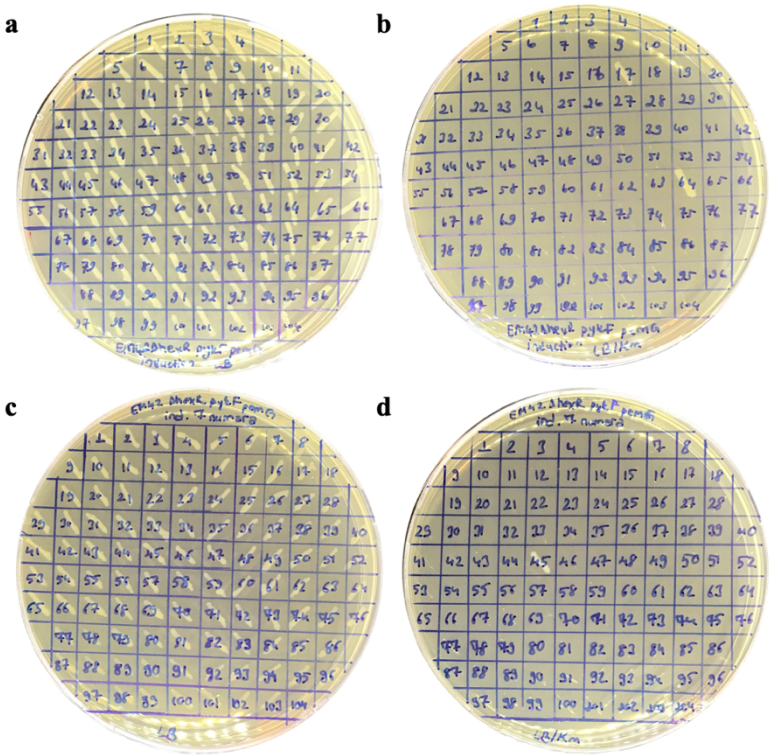

Figure 4.18: Re-streaked the colonies onto LB and LB-Km plates after induction. (a) Re-streaking of the colony 2 on an LB agar after induction. (b) Re-streaking of the colony 2 on an LB-Km plate after induction. (c) Re-streaking of the colony 7 on an LB agar after induction. (d) Re-streaking of the colony 7 on an LB-Km plate after induction.

Many colonies sensitive to Km were selected and screened by colony PCR. Colony PCR was performed using the P5-P8 primers to check Km-sensitive colonies derived from the induction of colony 7. The 1.5 kb band was observed only in colony 12, while the other colonies exhibited a 3 kb band, indicating that these colonies are revertant to the wild type (Figure 4.19). Deletion of the *pykF* gene was also confirmed using P15-P16 primers (Figure 4.25), resulting in the successful generation of the *P. putida* ΔXF strain.

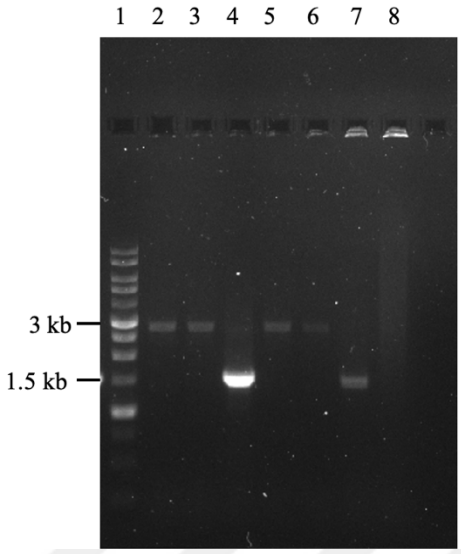

Figure 4.19: Image of an %1 agarose gel showing colony PCR result for Km-sensitive colonies with P5-P8 primers after induction. 1: marker (1kb DNA Marker, Ecotech); 2-6: PCR product of 10-14 colonies; 7: induced colony; 8: *P. putida* EM42.

4.2.3. Deletion of *pykF* gene from *P. putida* EM42Δ*hexR*Δ*pykA* Strain

Following successful sequencing and confirmation through colony PCR, *E. coli* DH5αλpir/pEMG-*pykF* colonies were selected for plasmid isolation. 200 ng of pEMG-*pykF* plasmid was transformed to the *P. putida* ΔXA strain by electroporation and plated into LB-Km. The presence of the pEMG-*pykF* plasmid was verified through colony PCR using P5-P8 primers after electroporation. A 1.5 kb band was not observed for colony 6 on the agarose gel (Figure 4.20.a). Colony PCR was repeated with P9-P10 primers (Figure 4.20.b), and colonies 4 and 8 were selected as recipient cells for conjugation.

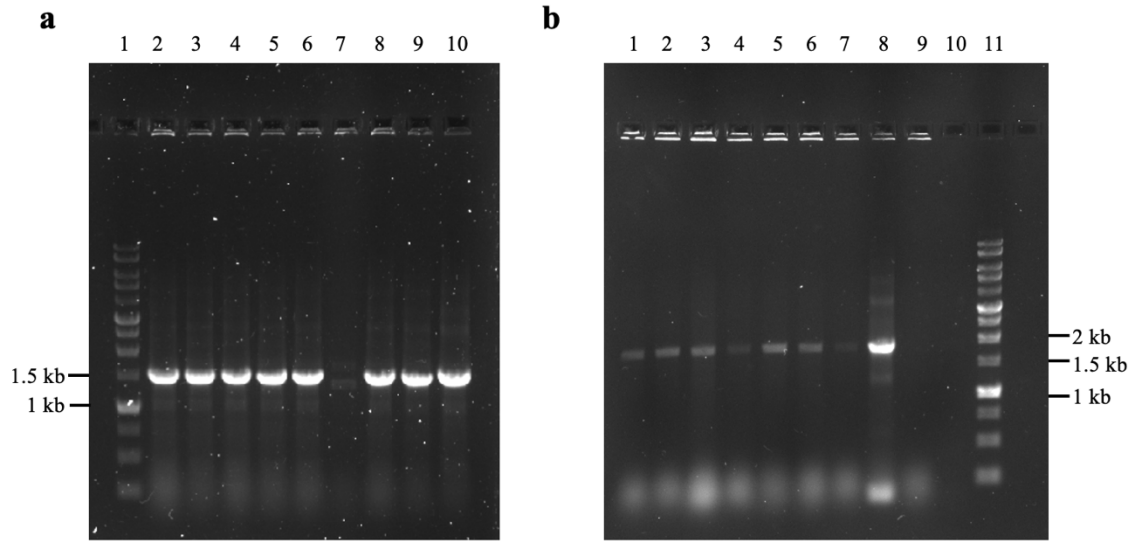

Figure 4.20: Image of an %1 agarose gel showing colony PCR results of pEMG-*pykF* plasmid electroporation to the *P. putida* ΔXA strain. (a) with P5-P8 primers. 1: marker (1kb DNA Marker, Ecotech); 2-9: 1-8 colonies; 10: pEMG-*pykF* plasmid (positive control). (b) with P9-P10 primers. 1-7: 1-5, 7, and 8 colonies; 8: pEMG-*pykF* plasmid (positive control); 9: *P. putida* EM42; 10: negative control (no DNA template); 11: marker (1kb DNA Marker, Ecotech).

Conjugation was performed to transfer the pSW-I plasmid to *P. putida* ΔXA/pEMG-*pykF* strain serving as the recipient cells and plated into Cetrimide-Amp. The green colonies were re-streaked and checked by colony PCR for the presence of pSW-I plasmid.

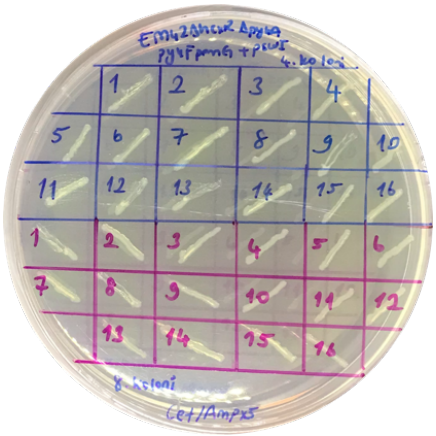

Figure 4.21: Re-streaking the *P. putida* ΔXA/pEMG-*pykF* + pSW-I colonies resulting from conjugation onto the Cet-Amp plate.

Colonies 12 and 13 from the conjugation using colony 4 as the recipient and colonies 1 and 8 from the conjugation using colony 8 as the recipient were screened with P5-P8, P9-P10, and P11-P12 primers. Only in colony 12, the 1.5 kb band was observed on agarose gel after colony PCR with P5-P8 primers (Figure 4.22.a). The presence of the pSW-I plasmid in the same colony was confirmed by observing a 520 bp band on the agarose gel (Figure 4.22.b). Therefore, only this colony was selected for the induction.

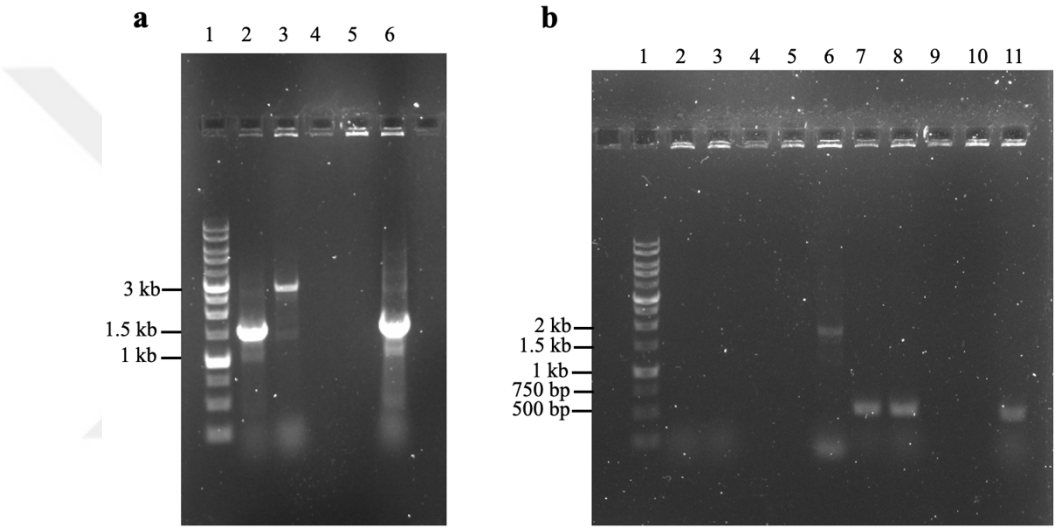

Figure 4.22: Image of an %1 agarose gel showing colony PCR results with P5-P8, P9-P10, and P11-P12 primers for the verification of conjugation pSW-I plasmid into *P. putida* ΔXA/pEMG-*pykF*. (a) with P5-P8 primers. 1: marker (1kb DNA Marker, Ecotech); 2, 3: colonies 12 and 13 from the conjugation using colony 4 as the recipient; 4, 5: colonies 1 and 8 from the conjugation using colony 8 as the recipient; 6: pEMG-*pykF* plasmid (positive control). (b) with P9-P10 and P11-P12 primers. 1: marker (1kb DNA Marker, Ecotech); 2, 3: colonies 12 and 13 from the conjugation using colony 4 as the recipient with P9-P10 primers; 4, 5: colonies 1 and 8 from the conjugation using colony 8 as the recipient with P9-P10 primers; 6: pEMG plasmid (positive control) with P9-P10 primers; 7, 8: colonies 12 and 13 from the conjugation using colony 4 as the recipient with P11-P12 primers; 9, 10: 1 and 8 from the conjugation using colony 8 as the recipient with P11-P12 primers; 11: *E. coli* DH5α/pSW-I (positive control) with P11-P12 primers.

The colony was induced overnight with 15 mM 3MB and diluted several times before being plated onto LB agar. The colonies were streaked simultaneously on LB and LB plates containing Km. While all colonies grew on the LB (Figure 4.23.a), they did not

grow on the LB-Km (Figure 4.23.b). Then, Km-sensitive colonies were further confirmed by colony PCR using P5-P8 primers (Figure 4.24). Further, colony PCR was done to confirm *P. putida* ΔXAF strain using P13-P14 and P15-P16 primers (Figure 4.25).

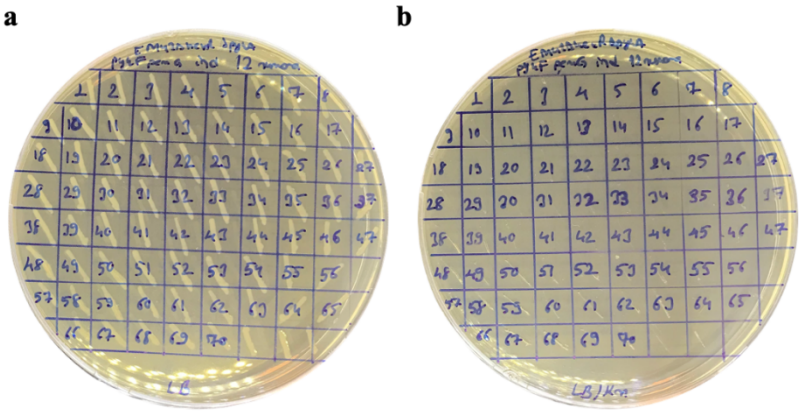

Figure 4.23: Re-streaked the *P. putida* ΔXA/pEMG-*pykF*+pSW-I colonies onto LB and LB-Km plates after induction.

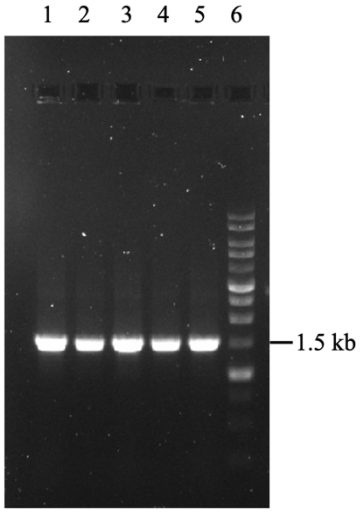

Figure 4.24: Image of an %1 agarose gel showing colony PCR result for Km-sensitive colonies with P5-P8 primers after induction. 1-5: 2-6 colonies; 6: marker (1kb DNA Marker, Ecotech).

The colony PCR was performed on the *P. putida* ΔXF and *P. putida* ΔXAF strains using P13-P14 and P15-P16 primers, with the wild-type strain *P. putida* EM42 as the positive control. Km-sensitive colonies 2 and 3 of *P. putida* ΔXFA and Km-sensitive 12 and 15 colonies of *P. putida* ΔXF were confirmed using the internal primers (Figure 4.25).

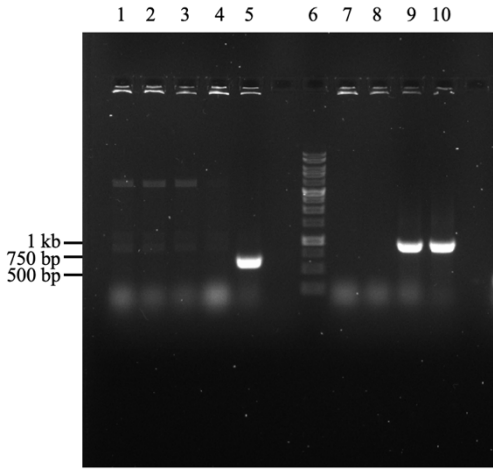

Figure 4.25: Image of an %1 agarose gel showing colony PCR result using P13-P14 and P15-P16 primers for the confirmation of successful deletions of the *pyk* genes in *P. putida* ΔX strain. 1, 2: Km-sensitive 2 and 3 colonies of *P. putida* ΔXAF using P15-P16 primers; 3, 4: Km-sensitive 12 and 15 colonies of *P. putida* ΔXF using P15-P16 primers; 5: *P. putida* EM42 using P15-P16 primers; 6: marker (1kb DNA Marker, Ecotech); 7,8: Km-sensitive 2 and 3 colonies of *P. putida* ΔXAF using P13-P14 primers; 9: Km-sensitive colony 12 of *P. putida* ΔXF using P13-P14 primers; 10: *P. putida* EM42 using P13-P14 primers.

No band was observed with the P15-P16 primers in *P. putida* ΔXF and *P. putida* ΔXAF strains, whereas a band was observed in the wild-type P. *putida* EM42 as expected. Colony PCR was performed with P13-P14 primers, and no band was detected in *P. putida* ΔXAF, while a band was observed in *P. putida* ΔXF and the wild-type *P. putida* EM42 at the same size.

Finally, all genome-edited strains stored in the -80 stock were tested again by colony PCR using P13-P14, P15-P16, and *hexR* primers (Figure 4.26). In the *P. putida* ΔXAF strain, no band was observed with either P13-P14 or P15-P16 primers, while in the *P. putida* ΔXF strain, a band was observed at 1 kb using the P13-P14 primers, similar to the wild-type *P. putida* EM42, but no band was detected with the P15-P16 primers. In the genome-edited strains screened with *hexR* primers, a band of different sizes was observed compared to the wild-type, as expected.

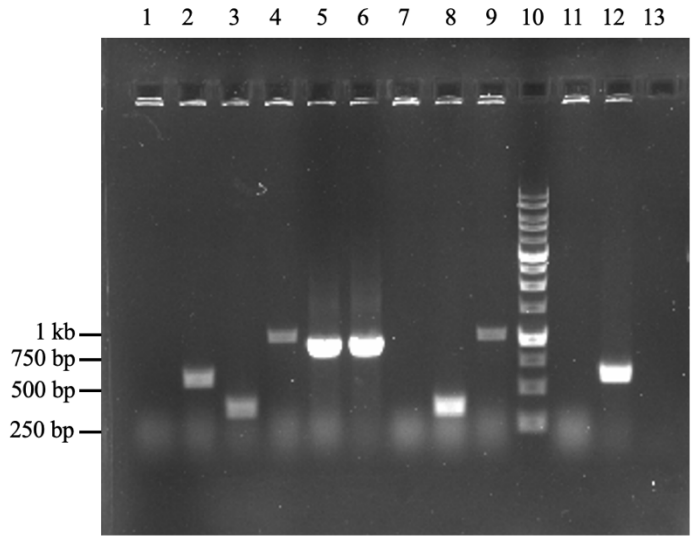

Figure 4.26: Image of an %1 agarose gel showing colony PCR results for genome-edited strains stored in the glycerol stock using *hexR*, P13-P14, and P15-P16 primers. 1, 2: *P. putida* ΔXF and *P. putida* EM42, respectively, using P15-P16 primers; 3, 4: *P. putida* ΔXF and *P. putida* EM42, respectively, using *hexR* primers; 5, 6, 7: *P. putida* ΔXF, *P. putida* EM42, and *P. putida* ΔXAF, respectively, using P13-P14 primers; 8, 9: *P. putida* ΔXAF and *P. putida* EM42, respectively, using *hexR* primers; 10: marker (1kb DNA Marker, Ecotech); 11, 12: *P. putida* ΔXAF and *P. putida* EM42, respectively, using P15-P16 primers; 13: negative control (no DNA template).

4.3. The Effect of *pyk* Gene Deletions on Cell Growth and Glucose Consumption in Genome Edited *P. putida* Strains

To determine the essentiality of *pykA* and *pykF* genes for growth, *P. putida* EM42, *P. putida* ΔX, *P. putida* ΔXA, *P. putida* ΔXF, *P. putida* ΔXAF strains were compared in M9 minimal media with starting OD_{600} set to 0.1. The strains were cultured for 72 h, and OD_{600} was measured at 6, 12, 18, 24, 36, 48, and 72 h intervals.

In the strain *P. putida* EM42, the OD_{600} of the cell 0.73, 1.37, 1.68, 2.04, 1.94, 1.85, and 1.95 at 6, 12, 18, 24, 36, 48, and 72 h intervals, respectively. The culture was in the logarithmic growth phase until 24 h, then entered the stationary until the end of 72 h of cultivation (Figure 4.27.a).

In the strain *P. putida* ΔX, the OD_{600} measurements of the cells at the specified time points were observed as 0.77, 1.17, 1.42, 1.83, 1.73, 1.7, and 1.54, respectively. After incubation

for 24 h, the culture was in a logarithmic growth phase followed by a stationary phase at 24 to 48 h and thereafter entered the death phase from 48 h to 72 h (Figure 4.27.b).

In the strain, *P. putida* ΔXF, the initial OD_{600} of the culture was set to 0.1 following 0.93, 1.56, 1.91, 2.12, 1.96, 2.01, and 1.90 at 6, 12, 18, 24, 36, 48, and 72 h intervals, respectively. The strain remained in the log phase for the first 24 h of incubation, followed by a stationary phase until the end of 72 h (Figure 4.27.c).

Interestingly, in the strain *P. putida* ΔXA, the OD_{600} was observed as 0.5, 0.95, 1.26, 1.41, 1.63, 2.02, and 1.93 at 6, 12, 18, 24, 36, 48, and 72 h intervals, respectively. It was observed that the log phase is extended to 48 h, followed by a stationary phase from 48 h to 72 h. The death phase was not observed within 72 hours (Figure 4.27.d).

In the strain, *P. putida* ΔXAF, the OD_{600} was observed as 0.46, 0.97, 1.2, 1.22, 1.50, 1.97, and 1.89 at 6, 12, 18, 24, 36, 48, and 72 h intervals, respectively. The cells continued to grow until the 18 h. Between 18 h and 24 h, their growth remained almost constant, reaching maximum growth at the 48 h. After the 48 h, the cells entered the stationary phase (Figure 4.27.e).

Although the *pyk*-deleted strains reached their maximum growth at different times and their logarithmic phases changed, they achieved similar OD_{600} values after 72 hours.

The bacterial growth rate of the strains is calculated by the following exponential growth formula (4.1) [Garay-Novillo et al., 2019]:

$$\mu = ln(ODt - OD0) / t \qquad (4.1)$$

OD_t is the optical density at time t.

OD_0 is the initial optical density.

The growth rates of the strains *P. putida* EM42, *P. putida* ΔX, *P. putida* ΔXF, *P. putida* ΔXA, and *P. putida* ΔXAF were 0.1144, 0.1071, 0.1138, 0.0497, 0.0489 h^{-1}, respectively. It was observed that the introduction of the *pykA* deletion slowed down the growth rate of the strains.

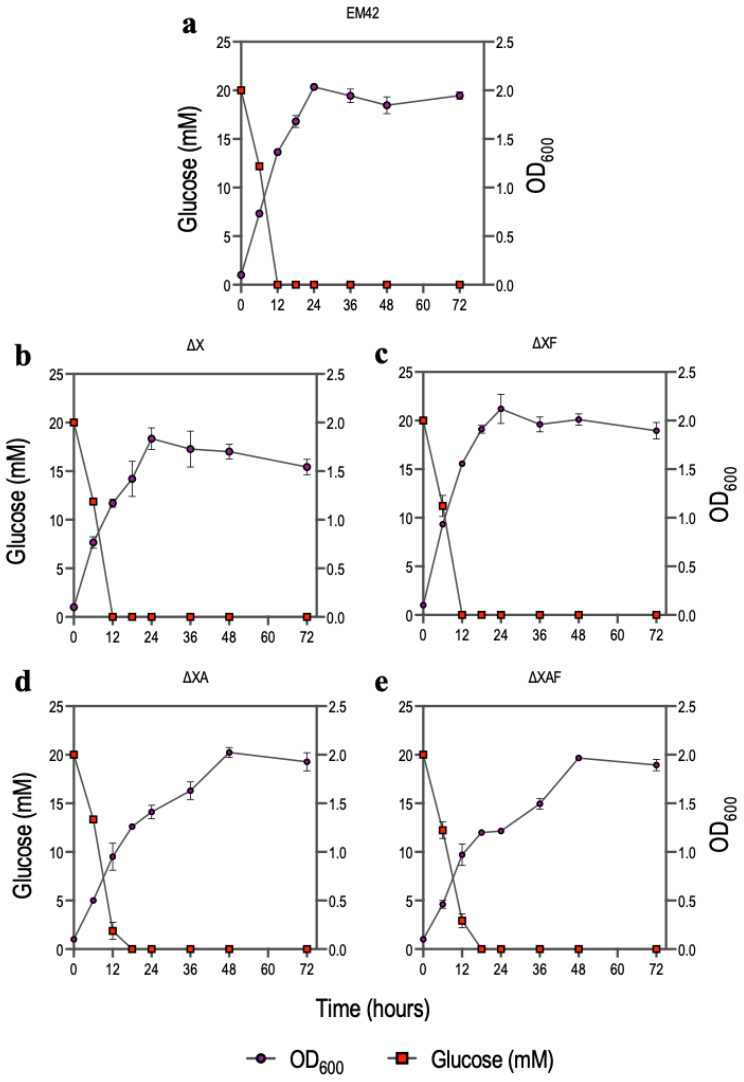

Figure 4.27: Growth profile and glucose consumption of the (a) *P. putida* EM42 (b) *P. putida* ΔX, (c) *P. putida* ΔXF, (d) *P. putida* ΔXA, and (e) *P. putida* ΔXAF strains grown for 72 h.

The glucose consumption of *P. putida* EM42*, P. putida* ΔX, *P. putida* ΔXF, *P. putida* ΔXA, and *P. putida* ΔXAF strains were analyzed by HPLC until the glucose was completely consumed.

In *P. putida* EM42 strain, the glucose was consumed within 12 h. The initial concentration of the glucose was 20 mM, which decreased to 12.18 mM, then completely consumed at 12 h. (Figure 4.27.a)

In *P. putida* ΔX, the glucose was consumed within 12 h. When the initial glucose concentration was 20 mM, it decreased to 11.86 mM at 6 h of cultivation, and all glucose was completely consumed at 12 h (Figure 4.27.b).

In *P. putida* ΔXF, also the glucose was consumed within 12 h. At 6 h of the cultivation, 11.21 mM glucose remained in the medium, then no glucose was detected at 12 h (Figure 4.27.c). As observed in **Figure 4.27**, the *P. putida* EM42, *P. putida* ΔX, and *P. putida* ΔXF strains exhibit a very similar profile in terms of glucose consumption.

In *P. putida* ΔXA, at 6, 12, and 18 hours, the glucose concentrations in the cell culture were 13.33 mM, 1.87 mM, and 0 mM, respectively (Figure 4.27.d). According to these results, the *P. putida* ΔXA strain consumed glucose more slowly compared to the *P. putida* ΔX and *P. putida* ΔXF strains.

In *P. putida* ΔXAF, glucose concentrations were 12.23 mM, 2.92 mM, and 0 mM at 6, 12, and 18 hours, respectively (Figure 4.27.e). The *P. putida* ΔX and *P. putida* ΔXF strains and *P. putida* ΔXA and *P. putida* ΔXAF strains show similar behavior in terms of growth profile and glucose consumption. According to these results, the growth and glucose utilization rates were reduced with the introduction of the *pykA* gene deletion.

4.4. The Effect of *pyk* Gene Deletions on pH in Genome Edited *P. putida* Strains

Genome-edited strains and wild-type *P. putida* EM42 strains were grown in an M9 minimal medium supplemented with 20 mM glucose as a carbon source for 72 h. The pH changes were monitored at 6, 12, 18, 24, 36, 48, and 72 h intervals.

In the *P. putida* EM42 strain, the initial pH was 7.24, and following 6.98, 6.73, 6.82, 6.84, 6.88, 6.98, and 7.05 at 6, 12, 18, 24, 36, 48, and 72 hours, respectively. pH decreased during the first 12 h of cultivation and then increased and approached neutral pH. (Figure 4.28.a).

In the *P. putida* ΔX strain, pH was initially 7.24 and measured as 6.96, 6.73, 6.83, 6.91, 6.95, 7.00, and 7.07 at 6, 12, 18, 24, 36, 48, and 72 hours, respectively. pH decreased sharply after incubation for 12 h. Subsequently, it gradually began to increase from 6.73 to 7.07 until the 72 h of cultivation (Figure 4.28.b).

In *P. putida* ΔXF, pH decreased before 12 h and began to increase from 6.73 to 7.08 until 72 h of cultivation. pH was measured as 7.24 initially and following 6.97, 6.73, 6.79, 6.89, 6.98, 6.99, and 7.09 at 6, 12, 18, 24, 36, 48, and 72 hours respectively (Figure 4.28.c).

In the strain *P. putida* ΔXA, pH decreased before 12 h, followed by almost constant until 18 h, and began to increase gradually from 6.77 to 7.07 until the end of incubation. pH was measured as 7.24 initially and following 7.03, 6.75, 6.77, 6.86, 6.91, 6.98, and 7.07 at 6, 12, 18, 24, 36, 48, and 72 hours, respectively (Figure 4.28.d).

In strain *P. putida* ΔXAF, the pH profile is highly similar to that of strain *P. putida* ΔXA. pH decreased before the 12 h, followed by almost constant until the 18 h, and began to increase gradually from 6.77 to 7.04 until the end of incubation. pH was measured as 7.22 initially and following 7.02, 6.80, 6.77, 6.83, 6.89, 6.98, and 7.04 at 6, 12, 18, 24, 36, 48, and 72 hours, respectively (Figure 4.28.e).

In all strains, an increase in pH was observed after 18 h, with the medium approaching neutrality.

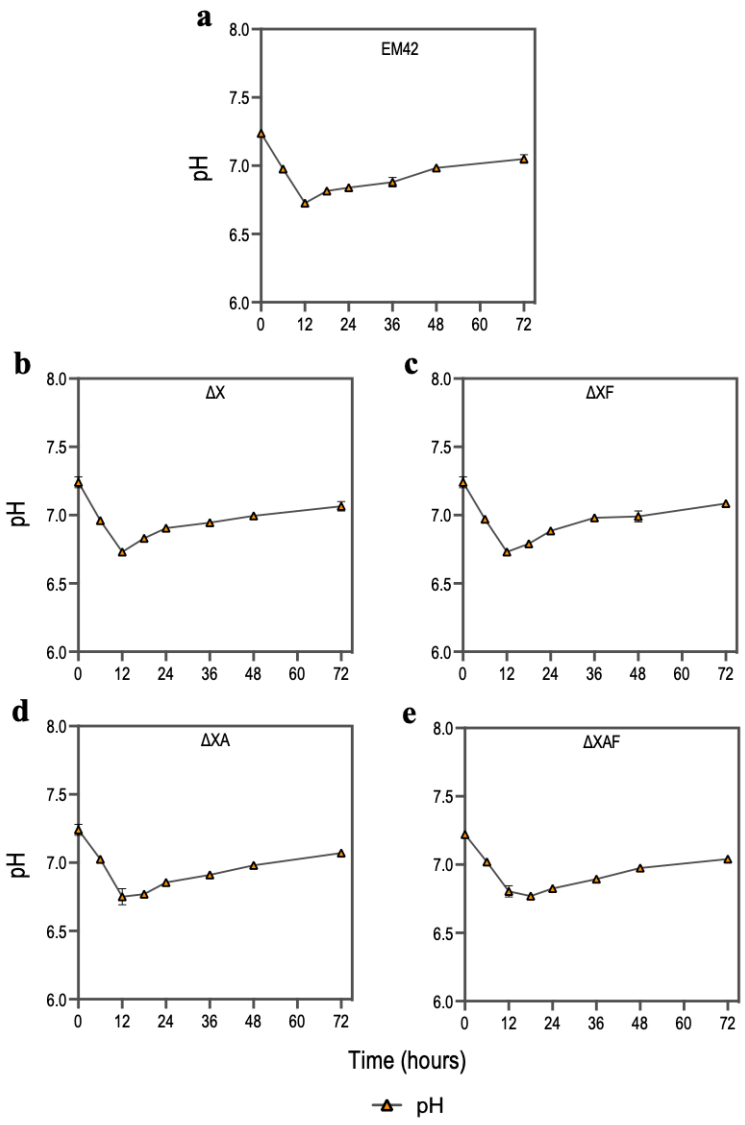

Figure 4.28: pH profile of the (a) *P. putida* EM42, (b) *P. putida* ΔX, (c) *P. putida* ΔXF, (d) *P. putida* ΔXA, and (e) *P. putida* ΔXAF strains cultivated for 72 h.

4.5. The Effect of *pyk* Gene Deletions on SA and DHS Production in Genome Edited *P. putida* Strains

Genome-edited strains and wild-type *P. putida* EM42 were cultivated in shake flasks in an M9 minimal medium containing 20 mM of glucose as the only carbon source for 72 h. Metabolite samples were collected every 24 h, and subsequently, concentrated samples were analyzed using an HPLC. The concentrations of DHS and SA metabolites were measured to elucidate the flux towards the SA pathway. The removal of *pykA* reduced the

conversion of PEP to pyruvate, thus increasing the pool of precursor for the SA pathway. Although the deletion of the *pykF* gene did not enhance flux as much as *pykA*, an increase in SA production compared to the *P. putida* ΔX as a reference strain was observed. Deletion of *pyk* genes at the same time resulted in the highest increase in flux towards the SA pathway among the genome-edited strains.

P. putida ΔXF strain led to the accumulation of 3.86, 9.70, and 10.12 ppm of DHS, 0.12, 0.5, and 0.95 ppm of SA at 24, 48, and 72 h, respectively. The production of DHS in the culture of *P. putida* ΔXF and SA production continued to increase for 72 h (Figure 4.29.a). *P. putida* ΔXA simultaneously led to the accumulation of 3.83, 9.78, and 10.2 ppm of DHS and 0.52, 0.83, and 1.44 ppm of SA at 24, 48, and 72 h, respectively. The production of DHS in the culture of *P. putida* ΔXA and SA synthesis continued to increase for 72 h, a higher level for SA production was observed compared to the *P. putida* ΔXF strain (Figure 4.29.b). Finally, in the *P. putida* ΔXAF strain, DHS has accumulated 3.97, 9.24, and 10.1 ppm, and SA accumulated 0.45, 1.03, and 1.70 ppm at 24, 48, and 72 h, respectively. DHS synthesis and SA flux in *P. putida* ΔXAF continued to increase for 72 h (Figure 4.29.c).

Figure 4.30 shows the fold change plot of SA concentrations relative to *P. putida* ΔX observed every 24 h for 72 hours. In the *P. putida* ΔXF strain, SA concentration increased by up to 1.06, 4.43, and 8.41-fold at 24, 48, and 72 h, respectively. In the *P. putida* ΔXA strain, 4.6, 7.34, and 12.74-fold increase in SA was observed at 24, 48, and 72 h, respectively. *P. putida* ΔXAF strain led to a 3.98, 9.11, and 15.04-fold enhanced SA accumulation compared to the initial strain. The introduction of the *pykA* deletion resulted in a higher fold change in SA production over 72 h compared to the *pykF* deletion.

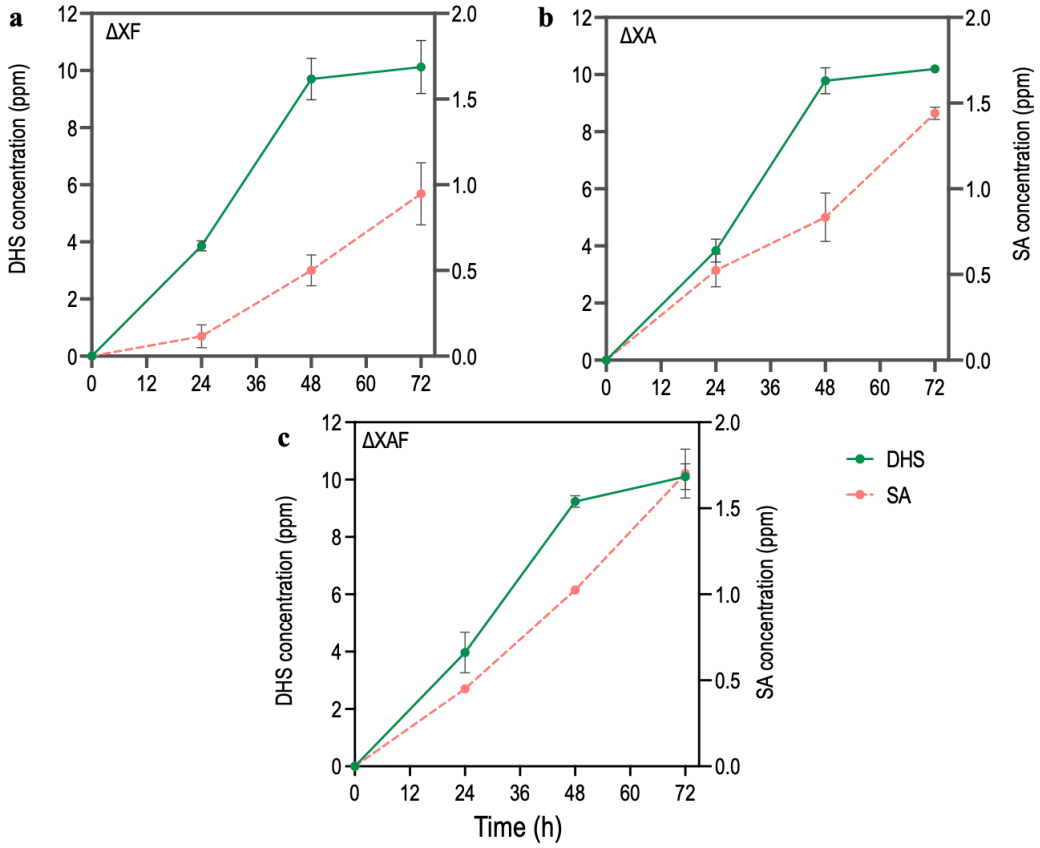

Figure 4.29: DHS and SA production of (a) *P. putida* ΔXF, (b) *P. putida* ΔXA, and (c) *P. putida* ΔXAF strains cultivated for 72 h.

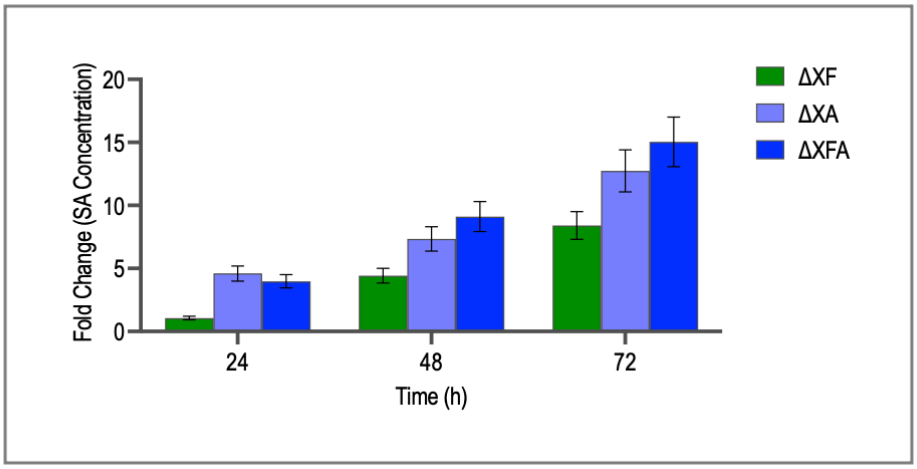

Figure 4.30: Change in SA concentration at 24, 48, and 72 hours of culture in *pyk*-deleted strains relative to the *P. putida* ΔX strain.

4.6. HPLC Analysis

4.6.1. Glucose Consumption Analysis by HPLC

HPLC was carried out to reveal glucose consumption profiles of the genome-edited strains and reference strain. Samples were collected at 6 h intervals from cultures grown in an M9 minimal medium containing an initial glucose concentration of 20 mM.

To construct the calibration curve, glucose standard samples of 30, 20, 10, 5, 2.5, and 1.25 mM concentrations were prepared by diluting them with an M9 minimal medium (Figure 4.31). Subsequently, these samples were analyzed using HPLC under specified experimental conditions. Peaks observed at the 6 min exhibited a proportional relationship with different glucose concentration standards.

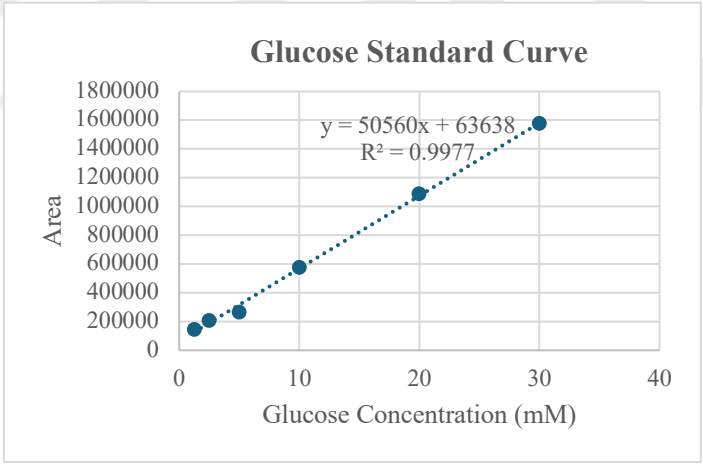

Figure 4.31: Glucose standard calibration curve was prepared at 30, 20, 10, 5, 2.5, and 1.25 mM concentrations.

4.6.2. Organic Acid Analysis by HPLC

The rotary evaporator (Figure 4.32) efficiently removes solvents under reduced pressure, thereby facilitating the concentration of extracted metabolites at controlled temperature and stirring conditions. The extraction protocol was performed at 40 °C, with a stirring speed of 150 rpm and a gradual pressure reduction from 850 mbar to 40 mbar. At this

point, the final volumes should be equal for all samples because, in the extraction process, they ensure comparability between samples, enhance analytical precision, allow for uniform evaluation of metabolite concentrations, standardize experimental conditions, and facilitate better interpretation of results.

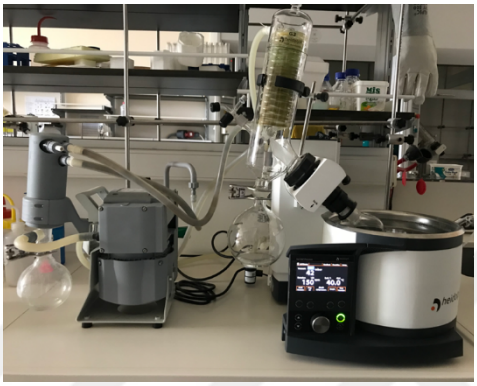

Figure 4.32: Setup for metabolite extraction using a rotary evaporator and vacuum pump.

HPLC was carried out to reveal the production of SA in both genome-edited strains and reference strain. The samples were collected at 24, 48, and 72 hours of the culture grown in an M9 minimal medium.

The calibration curve was constructed with SA standards at 2, 1.5, 1, 0.5, 0.3, and 0.1 ppm concentrations prepared in Milli-Q water and analyzed using the HPLC system under specified conditions (Figure 4.33). The peaks observed at 10.9 min showed proportional relationships between different concentrations of the standards.

DHS calibration curve was constructed at 100, 50, 25, 12.5, 6.25, and 3.1 µg/ml concentrations prepared in Milli-Q water and analyzed using the HPLC system under specified conditions. The peak was detected at 8.7 min. Different concentrations of the standards have proportional relationships to each other.

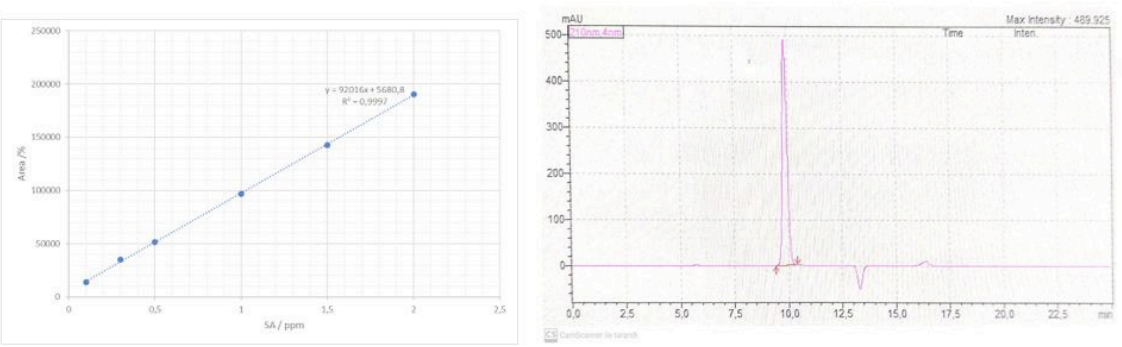

Figure 4.33: SA standard calibration curve was prepared using pure SA standards at different concentrations.

5. DISCUSSION

Within the scope of the thesis, we investigated how the deletion of *pykA* and *pykF* genes separately and together in the *P. putida* ΔX platform affects the metabolic flux from the PEP to the AAA pathway through the production of the SA metabolite.

The research also focused on analyzing how these genetic modifications altered the dynamics of cell growth when glucose serves as the sole carbon source. In addition, the biosynthesis of one of the key metabolite DHS within the SA pathway was thoroughly evaluated to understand the broader implications of *pyk* deletions on overall metabolic flux.

As bioinformatics analysis, the amino acid sequences of PykA and PykF from *P. putida* KT2440, *P. taiwanensis*, *P. aeruginosa*, *E. coli*, *S. typhimurium*, *Y. pestis*, *M. tuberculosis* were aligned using the ClustalOmega tool and average distances from percentage sequence identity were calculated. PykA and PykF were separated into two distinct groups in the phylogenetic tree. When comparing the amino acid sequences of the PykF protein across different organisms, it is observed that *P. putida* and *P. taiwanensis* are the most closely related with a similarity of over 98% in both enzymes. *P. aeruginosa* is more closely related to these two species. *E. coli* and *S. typhimurium* are more distant relatives to each other, followed by their nearest relative, *Y. pestis*. This pattern of relatedness is also true for the PykA protein. In *M. tuberculosis*, there is only one Pyk, and in terms of similarity, it comes after *P. aeruginosa* PykF protein.

In the study conducted by Ponce et al. (1995), the relative roles of two *pyk*s in *E. coli* have been revealed. They concluded that, although both *pykF* and *pykA* genes are actively involved in pyruvate biosynthesis, the enzyme PykF exhibits 15-fold higher activity compared to PykA when glucose serves as the only carbon source for cellular growth. The same study also reported that mutations in one or both *pyk* genes affect cell growth kinetics in *E. coli* when glucose is used as the sole carbon in the medium, and the most significant effect of deletions on bacterial growth is in the strain carrying the double mutant. However, it has been reported that *pyk* mutants reach the same final optical density at the end of the culture as the parental strain. This was explained to be due to the coordination

of the PTS (phosphotransferase transport system) and two pyruvate kinase enzymes to maintain a very low level of PEP, an allosteric regulator of several glycolytic enzymes and thus an important intermediate in pyruvate and glucose 6-phosphate biosynthesis. In this thesis, although the deletion of *pyk* genes caused a relative change in the exponential growth phase of the genome-edited strain compared to the parental strain, a similar growth rate to the parental strain was reached at the end of 72 hours.

In addition, in this study, deletion of the *pykA* gene caused a more dramatic negative effect on exponential-phase growth compared to parental strain. The amino acid sequences of the PykA proteins from *E. coli* and *P. putida* KT2440 revealed a similarity rate of 56.1%, while the PykF proteins showed a lower similarity of 37.1%. These results suggest that the Pyk in these two organisms differ significantly in both their aa sequences and likely their functional properties in the cell.

The growth kinetics of *P. putida* EM42 and genome-edited strains offer valuable insights into the metabolic pathways that govern cellular efficiency. The wild-type strain, *P. putida* EM42, exhibited the highest growth rate at 0.1144 h^{-1} in the exponential phase, providing a baseline for evaluating the effect of genetic alterations. The slight decrease in growth rate observed in the *P. putida* ΔX strain (6.38% reduction in exponential phase) suggests that the deletion of the *hexR* gene has a moderate effect on overall cellular growth compared to the wild-type strain. Furthermore, *P. putida* ΔX strain is accepted as a reference strain, and the effect of *pyk* genes on growth rate was investigated. *P. putida* ΔXF strain displayed a marginal increase in growth rate of about 6.26% compared to the reference strain. However, more significant reductions were observed in the strains *P. putida* ΔXA and *P. putida* ΔXAF, corresponding to substantial decreases of 53.59% and 54.34% compared to the reference strain in the exponential phase.

These results are similar to those reported in the study performed by Abdelhamid, (2019) on *P. aeruginosa* PA01. It was demonstrated that the deletion of *pykA* as in PW8308 ($pykA^-$ $pykF^+$) and PAF0 ($pykA^-$ $pykF^-$), grown in liquid media containing glucose resulted in reduced growth rates compared with the wild-type or PW3705 ($pykA^+$ $pykF^-$). Moreover, the PAF0 strain exhibited the slowest growth rate. However, they supported that PW3705 (only *pykF* deleted strain) displayed a slight growth impairment, showing that *pykF* also

seemed to have little effect, but in this study, the deletion of *pykF* slightly increased the growth rate when glucose was utilized as a carbon source. This may be because of differences between the reference strains. When comparing the aa sequences of Pyk enzymes in *P. aeruginosa* and *P. putida* KT2440, over 75% similarity was observed, and the deletion of both genes encoding these enzymes led to similar effects on the growth rates, indicating similar outcomes in both species.

Liu et al. (2016) utilized *Pseudomonas chlororaphis* GP72, isolated from the rhizosphere of green pepper, to produce three key antifungal compounds: 2-hydroxyphenazine (2-OH-PHZ), 2-hydroxy-phenazine-1-carboxylic acid (2-OH-PCA), and phenazine-1-carboxylic acid (PCA). Chorismate-derived compound PCA acts as a substrate of the phenazine derivatives. They target to suppress the gene *pykF* and obtain the mutant strain GP72Δ*pyk* that redistributes the metabolic flux in the central metabolism. They support that unlike the simultaneous disruption of both *pyk* genes, individually inactivating either the *pykA* or *pykF* gene could potentially increase the amount of PEP available for DAHP synthesis. After fermentation and HPLC analysis, the production of 2-OH-PHZ by GP72Δ*pyk* showed a 6.7-fold increase compared to GP72. Deleting this gene had minimal impact on bacterial growth without changing the exponential phases of wild-type and mutant strains. Contrary to these findings, our study demonstrates that the deletion of the *pykA* gene has an undeniable impact on the metabolic flux through the shikimate pathway. Also, the production of SA by the *pykF* deleted strain showed an 8.41-fold increase compared to the reference strain.

Previous studies have shown that deleting either *pykA* or *pykF* in *E. coli* resulted in only a slight improvement in DAHP levels, whereas the strain with both mutations showed a significant increase in titer [Huccetogullari et al., 2019]. In comparison to *E. coli*, Wynands et al. (2018) observed that the Δ*pykA* strain of *P. taiwanensis* VLB120 exhibited slowed growth in the medium supplemented with 20 mM glucose. It was confirmed (personal communication) that the Δ*pykA* strain showed a growth rate reduction of roughly 20% in a minimal medium with glucose as a sole carbon source and without vitamins or amino acids. In *P. taiwanensis* VLB120 the *pykA* inactivation enhanced phenol production. Further additional deletion of *pyk* resulted in no noticeable increase in production. In contrast, in our study, we observed that the addition of *pykF* deletion to

pykA significantly increased SA production. The difference in results may be due to branching in the metabolic pathway leading to phenol biosynthesis.

Li et al. (2021) analyzed the contributions of *pykA* and *pyk* to DAHP production in *P. putida* KT2440. By knocking out the *pykA* gene (strain PCA08) and *pyk* gene (strain PCA07), they aimed to demonstrate the distinct roles of these genes through shake flask fermentation experiments. Strain PCA08 produced 1.1 g/L of PCA, which was 1.2-fold and 2.7-fold higher than PCA07 and reference strain, respectively. Compared to *pyk*, the *pykA* gene enhanced the metabolic flow toward product biosynthesis derived from the SA pathway. These findings suggested that *pykA* is a key bottleneck in the biosynthesis of PCA and plays a more significant role compared to *pyk*. In this study, in terms of SA production, *P. putida* ΔXA strain was 1.5-fold and 12.74-fold higher than *P. putida* ΔXF and reference strain, respectively. Although these results confirm that *pykA* is the main player in the metabolic flow from the PEP to the AAA pathway, the role of *pykF* also cannot be negligible.

Bentley et al. (2020) suggest that the deletion of the transcriptional repressor gene *hexR* in *P. putida* KT2440 enhances both growth rate and muconate production. However, Bujdoš et al. (2023) demonstrate that the deletion of *hexR* in *P. putida* EM42 does not restore rapid growth in glucose. They argue that the differences between the *P. putida* KT2440 strain and the *P. putida* EM42 recombinant strain must be considered in this context. In this study, we also found that there is no significant difference in growth rate, and production of SA and DHS metabolites between the *hexR*-deleted *P. putida* EM42 strain and the wild-type strain.

The pH of the growth medium is crucial for bacteria as it directly affects enzyme activity, nutrient solubility, membrane transport processes, and overall metabolic efficiency, thereby maintaining cellular homeostasis. Deviations from the ideal pH can lead to denaturation of proteins, impaired growth, and even cell death. Therefore, controlling the pH of the medium is essential for maximizing bacterial growth and productivity. In this study, pH variations in genome-edited strains were monitored at specified time intervals. A drop in pH was observed during the first 12 h of cultivation in all strains, but by the end of 72 h, the pH gradually approached neutral values. After 72 h, the pH across all strains

ranged between 7.04 and 7.09, which is a desired and advantageous situation. It was shown that a sharp decrease in pH together with a decline in cell growth rate during the fermentation process for PCA production because of an acidic environment in the medium [Li et al., 2021]. This study did not encounter an acidification problem in the culture medium. Therefore, sustaining a pH-neutral fermentation environment could provide an advantage for the biosynthesis of various organic acids.

When comparing glucose consumption among the strains from samples taken every 6 hours, it was observed that the deletion of the *pykA* gene resulted in a slower rate of glucose consumption compared to the *pykF* gene deletion, reference strain (ΔX), and wild-type strain. In the study by Sawada et al. (2010) on *C. glutamicum* ATCC 13032, deletion of the *pyk* gene resulted in an increase in glucose consumption rate in the mutant strain. In contrast, a significant reduction in glucose consumption rate was detected in the *pyk*-deleted mutant of *B. subtilis* Fry et al. (2000). In our study, while the *pykF*-deleted strain did not cause any change in the glucose consumption rate compared to the reference strain, the *pykA*-deleted strain led to a slowdown in glucose consumption, similar to what was observed in *B. subtilis*.

The HPLC analysis revealed that SA production continued throughout the 72-hour period in all genome-edited strains. SA biosynthesis was slightly increased in the *P. putida* ΔXF strain, while the deletion of *pykA* led to a more significant improvement in the production. Finally, the most significant increase in the concentration of SA was obtained in *P. putida* ΔXAF strain in which both genes were deleted.

Additionally, the analysis of DHS production over 72 h, with measurements taken every 24 hours for the genome-edited strains, indicated that the production remained stable after 48 h in all evaluated strains. Interestingly, even though the DHS concentrations were consistent across the strains, the SA production continued throughout the 72-h period, along with the distinct production levels observed between the strains. Li et al. (2023) reported an engineered system for improved SA production in *E. coli*. They noticed that DHS accumulation may be caused by inadequate expression of *aroE* or by hydroaromatic equilibration. Then, they concluded that the DHS accumulation is due to the hydroaromatic equilibration. AroE enzyme can reduce SA to generate DHS, thus causing

the accumulation of DHS. The conversion of AroE to DHS and shikimate in *E. coli* were reported at rates of 17.5% and 77.5%, respectively. While such a mechanism has not yet been clarified in the *P. putida* EM42 strain in the literature, the stable DHS concentration along with increased SA production observed in our study indicates a potential hydroaromatic equilibration between these two metabolites.

In conclusion, *P. putida* is widely utilized in synthetic biology and metabolic engineering due to its ability to host pathways for chemical production or pollutant degradation. In this study, for the first time, the impact of *pyk* gene deletions, both individually and in combination, on the metabolic flux toward the AAA pathway was explored in a *hexR*-deleted *P. putida* EM42 strain. Using the I-SceI method for genome editing, the results indicated that the deletion of *pykA* reduced growth rate and glucose consumption, while significantly increasing flux towards the SA pathway compared to *pykF*. Furthermore, the simultaneous deletion of *pykA* and *pykF* resulted in the highest production of SA. These findings highlight the prevalent role of *pykA* in metabolic flux regulation and provide valuable insights into the function of *pyk* genes in *P. putida* players in directing the metabolic flux from PEP toward the AAA pathway.

REFERENCES

Abdelhamid, Y. (2019). “Two isoforms of pyruvate kinase enzymes in *Pseudomonas aeruginosa* with distinct functional and structural properties”.

Abdelhamid, Y., Brear, P., Greenhalgh, J., Chee, X., Rahman, T., & Welch, M. (2019). “Evolutionary plasticity in the allosteric regulator-binding site of pyruvate kinase isoform PykA from *Pseudomonas aeruginosa*”. *Journal of Biological Chemistry*, *294*(42), 15505–15516. doi: 10.1074/jbc.RA119.009156

Al Zaid Siddiquee, K., Arauzo-Bravo, M. J., & Shimizu, K. (2004). “Metabolic flux analysis of *pykF* gene knockout *Escherichia coli* based on 13C-labeling experiments together with measurements of enzyme activities and intracellular metabolite concentrations”. *Applied Microbiology and Biotechnology*, *63*(4), 407–417. doi: 10.1007/s00253-003-1357-9

Alcántara, A. R., Hernaiz, M. J., & Sinisterra, J. V. (2011). “Biocatalyzed Production of Fine Chemicals”. In Comprehensive Biotechnology, Second Edition (Vol. 3, pp. 309–331). Elsevier Inc. doi: 10.1016/B978-0-08-088504-9.00225-7

Babu, T., Yun, E. J., Kim, S., Kim, D. H., Liu, K. H., Kim, S. R., & Kim, K. H. (2015). “Engineering *Escherichia coli* for the production of adipic acid through the reversed β-oxidation pathway”. *Process Biochemistry*, *50*(12), 2066–2071. doi: 10.1016/j.procbio.2015.09.018

Bagdasarian, M., Lurz, R., Rückert, B., Franklin, F., Bagdasarian, M., Frey, J., & Timmis, K. (1981). “Specific-purpose plasmid cloning vectors II. Broad host range, high copy number, RSF 1010-derived vectors, and a host-vector system for gene cloning in *Pseudomonas*”. *Gene*, *16*(1–3), 237–247.

Bentley, G. J., Narayanan, N., Jha, R. K., Salvachúa, D., Elmore, J. R., Peabody, G. L., Black, B. A., Ramirez, K., De Capite, A., Michener, W. E., Werner, A. Z., Klingeman, D. M., Schindel, H. S., Nelson, R., Foust, L., Guss, A. M., Dale, T., Johnson, C. W., & Beckham, G. T. (2020). “Engineering glucose metabolism for enhanced muconic acid production in *Pseudomonas putida* KT2440”. *Metabolic Engineering*, *59*, 64–75. doi: 10.1016/j.ymben.2020.01.001

Blatny, J. M., Brautaset, T., Winther-Larsen, H. C., Karunakaran, P., & Valla, S. (1997). Improved Broad-Host-Range RK2 Vectors Useful for High and Low Regulated Gene Expression Levels in Gram-Negative Bacteria. In PLASMID (Vol. 38).

Bujdoš, D., Popelářová, B., Volke, D. C., Nikel, P. I., Sonnenschein, N., & Dvořák, P. (2023). “Engineering of *Pseudomonas putida* for accelerated co-utilization of glucose and cellobiose yields aerobic overproduction of pyruvate explained by an upgraded metabolic model”. *Metabolic Engineering*, *75*, 29–46. doi: 10.1016/j.ymben.2022.10.011

Chavadi, S., Wooff, E., Coldham, N. G., Sritharan, M., Hewinson, R. G., Gordon, S. V., & Wheeler, P. R. (2009). “Global effects of inactivation of the pyruvate kinase gene in the *Mycobacterium tuberculosis* complex”. *Journal of Bacteriology*, *191*(24), 7545–7553. doi: 10.1128/JB.00619-09

Chen, Y. Y., Galloway, K. E., & Smolke, C. D. (2012). “Conceptual frameworks for biological design Synthetic biology: advancing biological frontiers by building synthetic systems”. In Genome Biology (Vol. 13). Retrieved from http://genomebiology.com/2012/13/2/240

Chung, C. T., Niemela, S. L., & Miller, R. H. (1989). “One-step preparation of competent *Escherichia coli*: Transformation and storage of bacterial cells in the same solution (recombinant DNA)”. In Biochemistry (Vol. 86).

Concepcion, G.-O., & Garrido-Pertierra, A. (1987). “Purification and kinetic properties of pyruvate kinase isoenzymes of *Salmonella typhimurium*”. In Biochem. J.

Conway, T. (1992). “The Entner-Doudoroff pathway: history, physiology and molecular biology”. *FEMS Microbiology Letters*, *103*(1), 1–28. doi: 10.1111/j.1574-6968.1992.tb05822.x

Fry, B., Zhu, T., Domach, M. M., Koepsel, R. R., Phalakornkule, C., & Ataai, M. M. (2000). “Characterization of Growth and Acid Formation in a *Bacillus subtilis* Pyruvate Kinase Mutant”. In APPLIED AND ENVIRONMENTAL MICROBIOLOGY (Vol. 66, Issue 9). Retrieved from https://journals.asm.org/journal/aem

Garay-Novillo, J. N., García-Morena, D., Ruiz-Masó, J. Á., Barra, J. L., & Del Solar, G. (2019). “Combining modules for versatile and optimal labeling of lactic acid bacteria: Two pMV158-family promiscuous replicons, a pneumococcal system for constitutive or inducible gene expression, and two fluorescent proteins”. *Frontiers in Microbiology*, *10*(JUN). doi: 10.3389/fmicb.2019.01431

García-Granados, R., Lerma-Escalera, J. A., & Morones-Ramírez, J. R. (2019). “Metabolic engineering and synthetic biology: Synergies, future, and challenges”. *Frontiers in Bioengineering and Biotechnology*, *7*(MAR). doi: 10.3389/fbioe.2019.00036

Hanahan, D. (1983). “Studies on Transformation of *Escherichia coli* with Plasmids”. In J. Mol. Biol (Vol. 166).

Hanahan, D., & Meselson, M. (1980). “Plasmid screening at high colony density (Recombinant DNA; bacterial colony hybridization; nitrocellulose filters; chloramphenicol amplication; colony storage)”. In Gene (Vol. 10).

Hattori, J., Baum, B. R., Mchugh, S. G., Blakeley, S. D., Dennist, D. T., & Miki, B. L. (1995). “Pyruvate Kinase Isozymes: Ancient Diversity Retained in Modern Plant Cells”. In Biochemical Systematic~ and Ecology (Vol. 23, Issue 7).

Hofmann, J., Heider, C., Li, W., Krausze, J., Roessle, M., & Wilharm, G. (2013). "Recombinant production of *Yersinia enterocolitica* pyruvate kinase isoenzymes PykA and PykF". *Protein Expression and Purification*, *88*(2), 243–247. doi: 10.1016/j.pep.2013.01.010

Huccetogullari, D., Luo, Z. W., & Lee, S. Y. (2019). "Metabolic engineering of microorganisms for production of aromatic compounds". *Microbial Cell Factories*, *18*(1). doi: 10.1186/s12934-019-1090-4

Kessler, B., de Lorenzo, V., & Timmis, K. N. (1992). "A general system to integrate lacZ fusions into the chromosomes of gram-negative eubacteria: regulation of the Pm promoter of the TOL plasmid studied with all controlling elements in monocopy" (Vol. 233).

Köbbing, S. (2020). "Development of synthetic biology tools for *Pseudomonas putida*" *APPLIED MICROBIOLOGY 23 Sebastian Köbbing Volume 23*. Retrieved from https://portal.dnb.de

Li, J., & Ye, B. C. (2021). "Metabolic engineering of *Pseudomonas putida* KT2440 for high-yield production of protocatechuic acid". *Bioresource Technology*, *319*. doi: 10.1016/j.biortech.2020.124239

Li, M., Liu, C., Yang, J., Nian, R., Xian, M., Li, F., & Zhang, H. (2020). "Common problems associated with the microbial productions of aromatic compounds and corresponding metabolic engineering strategies". In Biotechnology Advances (Vol. 41). Elsevier Inc. doi: 10.1016/j.biotechadv.2020.107548

Li, Z., Gao, C., Ye, C., Guo, L., Liu, J., Chen, X., Song, W., Wu, J., & Liu, L. (2023). Systems engineering of *Escherichia coli* for high-level shikimate production. *Metabolic Engineering*, *75*, 1–11. doi: 10.1016/j.ymben.2022.10.010

Lin, Y., Sun, X., Yuan, Q., & Yan, Y. (2014). "Extending shikimate pathway for the production of muconic acid and its precursor salicylic acid in *Escherichia coli*". *Metabolic Engineering*, *23*, 62–69. doi: 10.1016/j.ymben.2014.02.009

Liu, D. F., Ai, G. M., Zheng, Q. X., Liu, C., Jiang, C. Y., Liu, L. X., Zhang, B., Liu, Y. M., Yang, C., & Liu, S. J. (2014). "Metabolic flux responses to genetic modification for shikimic acid production by *Bacillus subtilis* strains". *Microbial Cell Factories*, *13*(1). doi: 10.1186/1475-2859-13-40

Liu, K., Hu, H., Wang, W., & Zhang, X. (2016). "Genetic engineering of *Pseudomonas chlororaphis* GP72 for the enhanced production of 2-Hydroxyphenazine". *Microbial Cell Factories*, *15*(1). doi: 10.1186/s12934-016-0529-0

Martínez-García, E., Calles, B., Arévalo-Rodríguez, M., & De Lorenzo, V. (2011). "PBAM1: An all-synthetic genetic tool for analysis and construction of complex bacterial phenotypes". *BMC Microbiology*, *11*. doi: 10.1186/1471-2180-11-38

Martínez-García, E., & de Lorenzo, V. (2011). “Engineering multiple genomic deletions in Gram-negative bacteria: Analysis of the multi-resistant antibiotic profile of *Pseudomonas putida* KT2440”. *Environmental Microbiology*, *13*(10), 2702–2716. doi: 10.1111/j.1462-2920.2011.02538.x

Martínez-García, E., & De Lorenzo, V. (2012). “Transposon-based and plasmid-based genetic tools for editing genomes of gram-negative bacteria”. *Methods in Molecular Biology*, *813*, 267–283. doi: 10.1007/978-1-61779-412-4_16

Martínez-García, E., Nikel, P. I., Aparicio, T., & de Lorenzo, V. (2014). “*Pseudomonas* 2.0: Genetic upgrading of *P. putida* KT2440 as an enhanced host for heterologous gene expression”. *Microbial Cell Factories*, *13*(1). doi: 10.1186/s12934-014-0159-3

Martins Dos Santos’, V. A. P., Timmis’ R’, K. N., Tummler’, B., & Weinel, C. (2004). “GENOMIC FEATURES OF *PSEUDOMONAS PUTIDA* STRAIN KT2440”.

Munoz, M. E., & Ponce, E. (2003). “Pyruvate kinase: current status of regulatory and functional properties”. *Comparative Biochemistry and Physiology Part B*, *135*, 197–218. doi: 10.1016/S1096-4959Ž03.00081-2

Nelson, K. E., Weinel, C., Paulsen, I. T., Dodson, R. J., Hilbert, H., Martins dos Santos, V. A. P., Fouts, D. E., Gill, S. R., Pop, M., Holmes, M., Brinkac, L., Beanan, M., DeBoy, R. T., Daugherty, S., Kolonay, J., Madupu, R., Nelson, W., White, O., Peterson, J., … Fraser, C. M. (2002). “Complete genome sequence and comparative analysis of the metabolically versatile *Pseudomonas putida* KT2440”. *Environmental Microbiology*, *4*(12), 799–808. doi: 10.1046/j.1462-2920.2002.00366.x

Nielsen, J. (2001). “Metabolic engineering”. In Applied Microbiology and Biotechnology (Vol. 55, Issue 3, pp. 263–283). doi: 10.1007/s002530000511

Nikel, P. I., Chavarría, M., Danchin, A., & de Lorenzo, V. (2016). “From dirt to industrial applications: *Pseudomonas putida* as a Synthetic Biology chassis for hosting harsh biochemical reactions”. In Current Opinion in Chemical Biology (Vol. 34, pp. 20–29). Elsevier Ltd. doi: 10.1016/j.cbpa.2016.05.011

Nikel, P. I., & de Lorenzo, V. (2018). “*Pseudomonas putida* as a functional chassis for industrial biocatalysis: From native biochemistry to trans-metabolism”. In Metabolic Engineering (Vol. 50, pp. 142–155). Academic Press Inc. doi: 10.1016/j.ymben.2018.05.005

Noor, E., Eden, E., Milo, R., & Alon, U. (2010). “Central Carbon Metabolism as a Minimal Biochemical Walk between Precursors for Biomass and Energy”. *Molecular Cell*, *39*(5), 809–820. doi: 10.1016/j.molcel.2010.08.031

Otto, & Maike. (2020). “Microbial catalysis of renewable resources into aromatics via the central metabolic precursor phenylalanine”. Aachen.

Pan, Z., Zhu, T., Domagalski, N., Khan, S., Koepsel, R. R., Domach, M. M., & Ataai, M. M. (2006). “Regulating expression of pyruvate kinase in *Bacillus subtilis* for control of growth rate and formation of acidic byproducts”. *Biotechnology Progress*, *22*(5), 1451–1455. doi: 10.1021/bp060049u

Poblete-Castro, I., Becker, J., Dohnt, K., Santos, V. M. Dos, & Wittmann, C. (2012). “Industrial biotechnology of *Pseudomonas putida* and related species”. In Applied Microbiology and Biotechnology (Vol. 93, Issue 6, pp. 2279–2290). doi: 10.1007/s00253-012-3928-0

Ponce, E., Noemi´flores, N., Martinez, A., Valle, F., Boli´var, F., & Boli´var, B. (1995). “Cloning of the Two Pyruvate Kinase Isoenzyme Structural Genes from *Escherichia coli*: the Relative Roles of These Enzymes in Pyruvate Biosynthesis”. In JOURNAL OF BACTERIOLOGY (Vol. 177, Issue 19). Retrieved from https://journals.asm.org/journal/jb

Rawat, G., Tripathi, P., & Saxena, R. K. (2013). “Expanding horizons of shikimic acid: Recent progresses in production and its endless frontiers in application and market trends”. In Applied Microbiology and Biotechnology (Vol. 97, Issue 10, pp. 4277–4287). doi: 10.1007/s00253-013-4840-y

Rose, I. A. (1970). ”Stereochemistry of pyruvate kinase, pyruvate carboxylase, and malate enzyme reactions”. *Journal of Biological Chemistry*, *245*(22), 6052–6056. doi: 10.1016/s0021-9258(18)62662-6

Sato, N., Kishida, M., Nakano, M., Hirata, Y., & Tanaka, T. (2020). “Metabolic Engineering of Shikimic Acid-Producing *Corynebacterium glutamicum* From Glucose and Cellobiose Retaining Its Phosphotransferase System Function and Pyruvate Kinase Activities”. *Frontiers in Bioengineering and Biotechnology*, *8*. doi: 10.3389/fbioe.2020.569406

Sawada, K., Zen-in, S., Wada, M., & Yokota, A. (2010). “Metabolic changes in a pyruvate kinase gene deletion mutant of *Corynebacterium glutamicum* ATCC 13032”. *Metabolic Engineering*, *12*(4), 401–407. doi: 10.1016/j.ymben.2010.01.004

Seeholzer, S. H., Jaworowski, A., & Rose, I. A. (1991). “Enolpyruvate: Chemical Determination as a Pyruvate Kinase Intermediate In Biochemistry” (Vol. 30).

Siddiquee, K. A. Z., Arauzo-Bravo, M. J., & Shimizu, K. (2004). “Effect of a pyruvate kinase (*pykF*-gene) knockout mutation on the control of gene expression and metabolic fluxes in *Escherichia coli*”. *FEMS Microbiology Letters*, *235*(1), 25–33. doi: 10.1016/j.femsle.2004.04.004

Sonoki, T., Takahashi, K., Sugita, H., Hatamura, M., Azuma, Y., Sato, T., Suzuki, S., Kamimura, N., & Masai, E. (2018). “Glucose-Free cis,cis-Muconic Acid Production via New Metabolic Designs Corresponding to the Heterogeneity of Lignin”. *ACS Sustainable Chemistry and Engineering*, *6*(1), 1256–1264. doi: 10.1021/acssuschemeng.7b03597

Tzin, V., Galili, G., & Aharoni, A. (2012). “Shikimate Pathway and Aromatic Amino Acid Biosynthesis”. In Encyclopedia of Life Sciences. Wiley. doi: 10.1002/9780470015902.a0001315.pub2

Voet, D., Voet, J. G., & Pratt, C. W. (2012). “Fundamentals of biochemistry: life at the molecular level”.

Waygood, E. B., Mort, J. S., & Sanwal, B. D. (1976). “The Control of Pyruvate Kinase of *Escherichia coli*. Binding of Substrate and Allosteric Effectors to the Enzyme Activated by Fructose 1,6-Bisphosphate”. Retrieved from https://pubs.acs.org/sharingguidelines

Weimer, A., Kohlstedt, M., Volke, D. C., Nikel, P. I., & Wittmann, C. (2020). “Industrial biotechnology of *Pseudomonas putida*: advances and prospects”. In Applied Microbiology and Biotechnology (Vol. 104, Issue 18, pp. 7745–7766). Springer. doi: 10.1007/s00253-020-10811-9

Wong, S. M., & Mekalanos, J. J. (2000). “Genetic footprinting with mariner-based transposition in *Pseudomonas aeruginosa*”. Retrieved from www.pnas.org

Wynands, B., Lenzen, C., Otto, M., Koch, F., Blank, L. M., & Wierckx, N. (2018). “Metabolic engineering of *Pseudomonas taiwanensis* VLB120 with minimal genomic modifications for high-yield phenol production”. *Metabolic Engineering*, *47*, 121–133. doi: 10.1016/j.ymben.2018.03.011

Yu, S. (2017). “Metabolic engineering and bio-electrochemical synthesis in *Pseudomonas putida* KT2440 for the production of p-hydroxybenzoate and 2-ketogluconate”.

Yu, S., Plan, M. R., Winter, G., & Krömer, J. O. (2016). “Metabolic engineering of *Pseudomonas putida* KT2440 for the production of para-hydroxy benzoic acid”. *Frontiers in Bioengineering and Biotechnology*, *4*(NOV). doi: 10.3389/fbioe.2016.00090

Zhu, Q., & Jackson, E. N. (2015). “Metabolic engineering of *Yarrowia lipolytica* for industrial applications”. In Current Opinion in Biotechnology (Vol. 36, pp. 65–72). Elsevier Ltd. doi: 10.1016/j.copbio.2015.08.010

BIOGRAPHY

Hatice ARSLAN went to Hacı Dudu Mehmet Gebizli Anatolian Imam Hatip High School. After she graduated, she went to Kadir Has University in the Department of Bioinformatics and Genetics in 2017. She graduated in 2022. Then, she began her master's education at Gebze Technical University, Molecular Biology and Genetics Department in 2022. Her postgraduate education continues.

PUBLICATIONS AND PRESENTATIONS FROM THE THESIS

Arslan H., Akkaya Ö., (2024), “Effect of Pyruvate Kinase in Enhancing Metabolic Flux to the Shikimate Pathway in *Pseudomonas putida*”, 1st International Congress on Biotech Solutions for Sustainability, Kocaeli/Gebze/Türkiye, May 8-10 2024